Applied Energy 293 (2021) 116826

Contents lists available at ScienceDirect

Applied Energy

journal homepage: www.elsevier.com/locate/apenergy

Energy and daylight performance of a smart window: Window integrated with thermotropic parallel slat-transparent insulation material

Yanyi Sun [a,*], Xin Liu [a], Yang Ming [a], Xiao Liu [a], Daniel Mahon [b], Robin Wilson [a], Hao Liu [a], Philip Eames [b], Yupeng Wu [a,*]

[a] Faculty of Engineering, University of Nottingham, Nottingham, UK
[b] Centre for Renewable Energy Systems Technology, Loughborough University, Loughborough, UK

HIGHLIGHTS

- TT PS-TIM smart window provides dynamic regulation of solar admission.
- Impacts of design factors of TT PS-TIM window on building performance are presented.
- Evaluated an office performance with TT PS-TIM window using an inclusive approach.
- Applying TT PS-TIM window results in energy saving of up to 27.1%.
- The TT PS-TIM window offers significant improvement in daylight performance.

ARTICLE INFO

Keywords:
Smart Window
Thermotropic Material
Parallel Slat Transparent Insulation Materials (PS-TIM)
Building Simulation
Building Energy Saving
Solar and Daylight Automatic Control

ABSTRACT

With the increasing awareness of building energy efficiency, indoor environment quality for human wellbeing and working efficiency, efforts have intensified in to inventing intelligent building components. This paper provides a first step in developing a novel multi-effect smart window system, which achieves enhanced energy efficiency and an improved indoor luminous environment by integrating a Transparent Insulation Material (TIM) structure incorporating a Thermotropic material. This system automatically regulates the admittance of solar heat and natural light into the building by responding to a changing environment while taking advantage of the increased thermal resistance and scattered daylight of window integrated TIM. A comprehensive workflow via EnergyPlus and RADIANCE was used to accurately predict the luminous and energy performance of applying the smart window system on a typical south-facing office under selected climates (London, Stockholm, Rome and Singapore). The effect of the optical properties and transition temperature of thermotropic material on building performance was explored in detail. Annual simulation results predict that, with a careful selection of the Thermotropic material properties, installing the TT PS-TIM window system is able to yield up to a 27.1% energy saving when compared with a conventional double glazed window, under the modelled Rome climate. TT PS-TIM windows also provide dynamic daylight control, resulting in increased daylight availability with the percentage of working hours that fall into the $UDI_{500\text{–}2000\ lx}$ range increasing to 62.3%. The results of this research provide guidance for the next step of the material design and development that seek to balance energy efficiency and solar and daylight control through the use of thermotropic materials.

1. Introduction

Buildings are responsible for one third of the worldwide GreenHouse Gas emissions (GHG) and 30–40% of the primary energy consumption [1,2]. In response to the international goals against climate change, numerous measures are set out to help improve the energy efficiency of buildings and reduce carbon emissions [3,4]. Windows in building envelopes are exceptionally important elements through which reduction in energy consumption and improvement of indoor comfort level can be achieved [5,6]. This is because windows contribute significantly to the heat gain and loss from a building's enclosure and determine the quantity, quality and distribution of daylight that penetrates into a space

* Corresponding authors.
E-mail addresses: Yanyi.Sun@nottingham.ac.uk (Y. Sun), Yupeng.Wu@nottingham.ac.uk (Y. Wu).

https://doi.org/10.1016/j.apenergy.2021.116826
Received 28 September 2020; Received in revised form 25 January 2021; Accepted 12 March 2021
Available online 21 April 2021
0306-2619/

[7,8].

One potential solution to improve the window performance is to apply a Transparent Insulation Material (TIM) into building windows [9]. TIM seeks to provide resistance to heat flow without hindering the transmittance of sunlight relative to a non-transparent insulation material. A lower thermal transmittance (i.e. U-value) of a TIM decreases undesired heat losses from the inside space to the external environment, and thus reduces the building's heating load [10,11]. Wong et al. [12] simulated the performance of TIM glazing that incorporated a 22 mm polymethyl methacrylate (PMMA) capillary slab on a south facing façade. The annual results they predicted for the climate of London showed that, when compared to standard double glazing, daytime internal temperature swings were reduced and up to a 6.1% heating energy saving in the winter could be achieved. Sun et al. [13] indicated that applying Parallel Slat TIM (PS-TIM) to a window of a typical small office led to a significant heating energy saving (i.e. 29%) when compared to double glazed windows if the HVAC system is in operation during both day-time and night-time, for the climate of London. If the HVAC system is only in operation during working hours, the heating energy saving potential predicted was 6.7%. The presence of TIM in windows also reduces solar transmittance (i.e. g-value or Solar Heat Gain Coefficient SHGC), leading to less solar heat transmitted into the room. This results in a reduced cooling load during hot weather [14,15] but increases the heating requirement in cold weather. Huang and Niu [14] predicted that translucent aerogel glazing systems installed in buildings in humid subtropical cooling-dominant climates (such as Hong Kong) could result in a 4% reduction of the total annual space cooling load when compared to conventional double glazing systems. In the research presented by Sun et al. [10], cooling was the dominant mechanism through which energy savings were made when integrating PS-TIM into building windows. An annual cooling saving potential of 34%, 15.9% and 11% were predicted for the climates of Beijing, Hong Kong and Singapore, respectively. Insertion of TIM material may also block and scatter daylight transmitted through the window [15,16]. This prevents strong direct daylighting and undesired glare, resulting in a more comfortable and uniform distribution of daylight into the occupied space and thus diminishes the requirement for shading devices [16]. The predictions from the studies by Sun et al. [10,13,16] indicated that the inclusion of PS-TIM systems improved the luminous environment by reducing the hours of over illumination and in so doing resulted in a more uniformed illumination of the working plane for different climates (i.e. Stockholm, London, Beijing, Hong Kong and Singapore). However, the reduced solar and visible transmittance also increased the predicted energy required for space heating and artificial lighting when the solar radiation and/or outdoor illuminance was low.

Novel switchable glazing is another potential system intended for application in buildings, providing the potential to improve both energy and daylighting performance [5,17,18]. This is achieved mainly through its ability to adjust solar and daylight transmittance in response to a varying external environment [19,20]. No matter what the stimuli, switchable glazing systems all have a minimum of two states, one before and one after switching [21,22]. The switching is triggered with the aim of: 1, blocking undesired solar radiation transmitted into the room and thus reducing the indoor temperature and corresponding cooling load [23]; 2, reducing strong natural sunlight and the potential for glare [24]; and 3, reducing transparency and increasing privacy. Thermotropic materials are a set of chromogenic substances within the switchable glazing range [25,26]. They provide a reversible adjustment in their light transmission behaviour from highly transparent to light diffusing in response to their temperature without the requirement of providing extra power [27]. Applying thermotropic materials to protect the overheating of solar absorbers [28,29] and in building windows to achieve active daylight control and energy consumption regulation has been investigated [30,31]. Yao and Zhu [32] investigated the indoor thermal environment, energy and daylighting performance of applying thermotropic double-glazed windows for the climate of Hangzhou, China through building simulation. They indicated that thermotropic double-glazed windows can reduce a buildings cooling energy demand by 19% and 3.6% of the total HVAC energy demand when compared with double-glazed windows, while providing an improved indoor illuminance condition with reduced possibility of glare [32]. Bianco et al [33] investigated the thermal and optical properties of a thermotropic glass pane in both laboratory and in-field tests. They concluded that the reduction of the solar and visual transmittance between the clear and the translucent state is around 20%.

Both of the techniques (TIM and TT) mentioned above provide the potential to achieve building energy conservation and daylight environment improvement. Although TIMs have U-values lower than that of traditional double glazing windows for better thermal insulation, with a transmittance varying between 10 and 40%, they have the potential to increase the artificial lighting energy consumption hence reducing the energy benefits. TT windows can control glazing spectral response, however, occupants' view communication with the external environment was totally blocked when the TT material was in its translucent state. To overcome the issues with traditional TIMs and TT windows, in this project we have developed a novel TT PS-TIM smart window system, which applies thermotropic (TT) material encapsulated within the slats of PS-TIM between the panes of double glazing windows (see Fig. 1a). The proposed TT PS-TIM smart window system provides both spatial tuning and real-time management of solar energy and daylight admission, achieves improved energy efficiency through increased thermal resistance as well as maintains external views. To be more specific, this proposed smart window provides automatic regulation of solar energy, which maximises the passive solar energy usage during winter and reduces buildings cooling energy demands during summer, offering a solution to help buildings reduce their emissions. However, questions related to the most desirable material features (e.g. transition temperature and optical properties) for its building application need to be addressed. Therefore, a comprehensive numerical model including thermal and optical modules for window and building simulation has been developed and perform a parametric analysis to explore the effects of the optical properties and transition temperatures of the thermotropic material on building energy performance and indoor luminous environment for selected climates. This work offers a first step in the development of a novel multi-effect smart window which aims to improve building energy efficiency and indoor comfort level. The results of this research provide guidance for the next step of the material design and development that aims to balance energy efficiency and solar and sunlight control using a thermotropic material.

2. Research Methodology:

In this research, a window unit integrated with TT PS-TIM was comprehensively investigated through a workflow that incorporates thermal and optical characterisation of proposed TT PS-TIM window systems and building simulation (i.e. EnergyPlus and RADIANCE) using a typical office space as a case study to explore the benefits of its implementation. Various optical properties and transition temperatures of the thermotropic layer were studied to explore and optimise the features for window applications. This section introduces the window design, testing scenarios, optical and thermal characterisation and building simulation methods.

2.1. TT PS-TIM prototype development and properties of the thermotropic material

Photos and schematic diagrams of the double-glazing unit integrated with the TT PS-TIM prototype are presented in Fig. 1(a) and (b). The double-glazing unit has a 15 mm air cavity between two glass panes. 15 mm wide, 1.5 mm thick slats are placed perpendicularly between glass panes, leaving no space between the slats' edges and the glass panes. The spacing between neighbouring slats is 10 mm. For each slat, a 0.5 mm

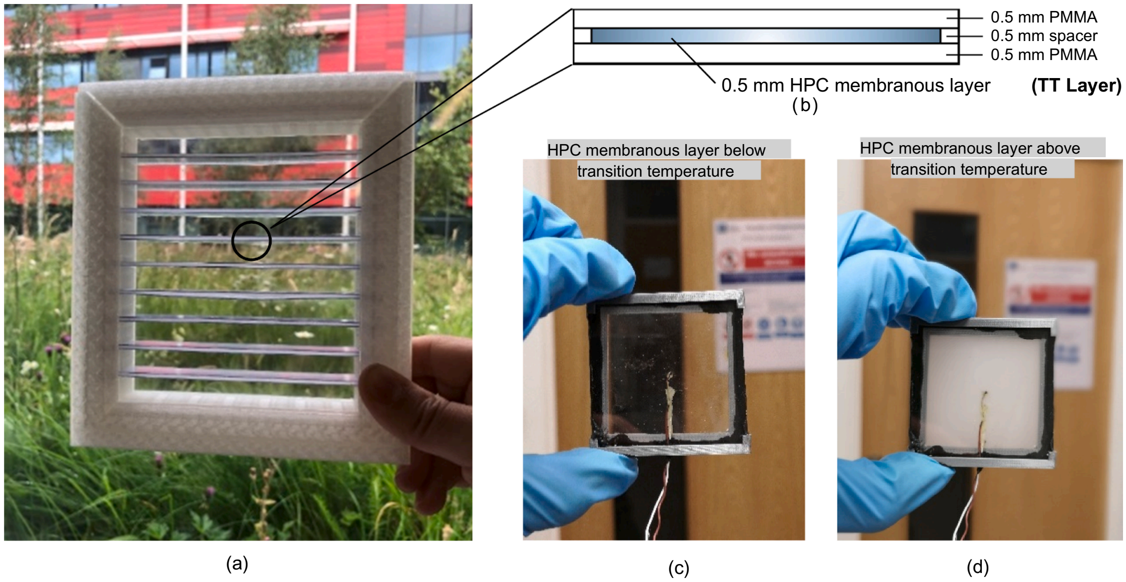

Fig. 1. (a) Picture of the window prototype with TT PS-TIM, (b) schematic diagram of the slat (not in scale) and (c) picture of the HPC membranous layer below transition temperature and (d) picture of the HPC membranous layer above transition temperature.

thermotropic membranous layer (TT layer) was sandwiched between two 0.5 mm PMMA sheets.

To develop the proposed TT layer, Hydroxypropyl cellulose (HPC), which was purchased in the form of an off-white powder from Sigma Aldrich (99% purity), was selected as the thermotropic membrane. The process of synthesising the HPC membranes can be found in previous publications [31] of the research group. HPC membranes with various molecular weight (e.g. 80 k Mw, 370 k Mw and 1,000 k Mw) and concentration (e.g. 1 wt%, 3 wt% and 5 wt%) have been synthesised for optical characterising.

The visible light and solar transmittance and reflectance of the slats, integrated with HPC membranes, around their transition temperature were measured using a spectrometer. Details of the measuring process and equipment used can be found in [31] and [34]. Fig. 2 demonstrates the variation of transmittance and reflectance of the HPC membrane with 370 k Mw 5 wt% along with the change of its temperature. It can be noticed that the HPC membrane has a high solar and visible transmittance above approximately 85% when its temperature is below its transition temperature (i.e. thermotropic membrane in its clear state). Once the temperature of the membrane is higher than its transition temperature (i.e. the thermotropic membrane is in its translucent state), the solar and visible transmittance dramatically drops to approx. 20% and the reflectance increases to approx. 35%. Photographs of the developed HPC thermotropic membrane in the transparent and translucent states can be seen in Fig. 1(c) and (d), respectively.

During the synthesising process, varying the TT materials' molecular weight or concentration, particle size and adding cosolvent or cross linker can alter the optical properties of a thermotropic membrane, in term of transmittance, reflectance and absorptance [13,19–21]. The transition temperature can also be regulated by the addition of salts or cosolvents and varying the concentration of the TT material [25,35,36]. However, questions over what is the optimum transition temperature and what features are most desirable for building applications are left unsolved. Answering the above questions requires consideration of various aspects, e.g. building form, function, location, local climate and occupant' behaviours. Numerically modelling a novel building component and conducting precise building simulations provides an economic approach to understanding the desired behaviours of the TT layer that enable improved building energy savings and increased daylight comfort. This information can then be fed back into the process of material design. Thus, in the following parts of this research, rather than employing the measured optical properties of all the currently under-

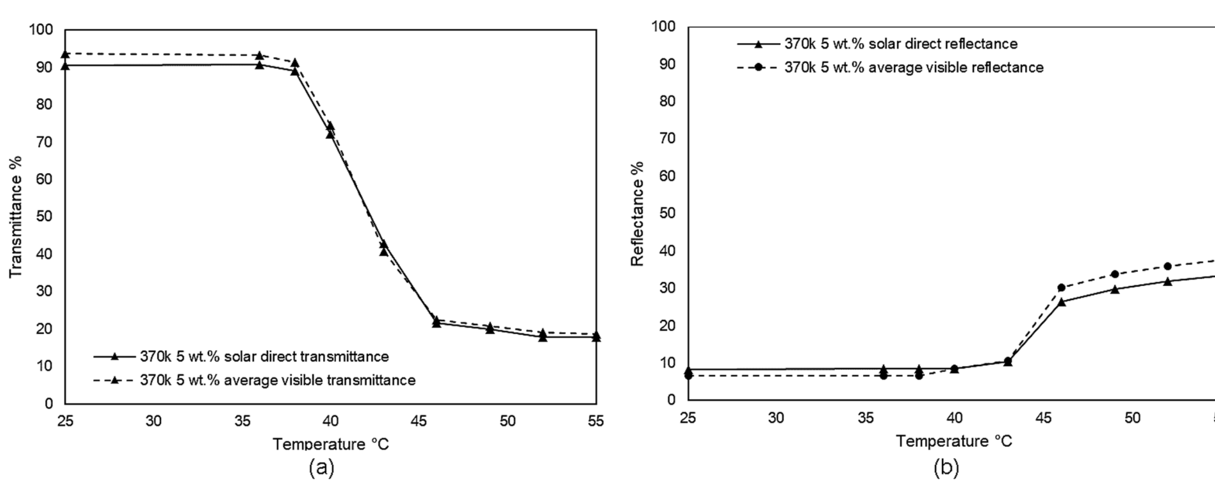

Fig. 2. Transmittance (a) and reflectance (b) of the developed HPC membrane with 370 k Mw and 5 wt%.

test materials, representative candidate window systems with theoretical properties, deduced based on the above experimental measurements shown in Fig. 2, were selected for inputs into the simulations. Specifically these properties were used in the numerical simulation to explore their effect on building energy demand and daylight comfort.

The transmittance, reflectance and absorptance of the candidate materials are shown in Table 1. Based on the measured optical properties of the thermotropic layer (0.5 mm 370 k 5 wt% HPC membrane), the TT membrane was assumed to have a high visible transmittance (i.e. approx. 85%) in its clear state (labelled as CS) at temperatures below its transition temperature. During the study, the clear state optical properties of the TT materials were kept unchanged and their translucent state (labelled as TS) optical properties varied. The first 4 specimens (i.e. #1, #2, #3 and #4), in their translucent state, have a reflectance of 35% while the transmittance increases from 10% to 40%, with a decrease of absorbance from 55% to 25% (see Table 1). For specimens #5, #2, #6 and #7, in their translucent state, the absorbance is 45% and the transmittance varies from 10% to 40% caused by the changing of the reflectance from 45% to 15%. Four transition temperatures (19 °C, 21 °C, 23 °C and 25 °C) were assumed in the modelling.

The TT PS-TIM are labelled as '$CS\text{-}TS_{t10r35}$', '$CS\text{-}TS_{t20r35}$', '$CS\text{-}TS_{t30r35}$', '$CS\text{-}TS_{t40r35}$', CS-TS_{t10r45}', 'CS-TS_{t30r25}' and 'CS-TS_{t40r15}' respectively and represent the TT material switching from CS to TS with different translucent-state optical properties. The assumed transition temperature (i.e. 19 °C, 21 °C, 23 °C and 25 °C) is added at the end of the label (e.g. '$CS\text{-}TS_{t20r35}\_25°C$'). In order to understand the mechanism by which savings were made, a window with clear PS-TIM (labelled as C PS-TIM) (i.e. slats with the same optical properties as the TT slats in their clear state) and windows with translucent PS-TIMs (labelled as T PS-TIMs) (i.e. slats with the same optical properties as the TT slats in their translucent state) were included for comparison.

2.2. Workflow of the research method

To explore the most desired features of the thermotropic material for its implementation in window integrated PS-TIM systems, a comprehensive approach, which consists of 4 major components, was used in this research and is illustrated in Fig. 3.

In the first phase, Computational Fluid Dynamics (CFD) software, Fluent (Version 15.0), was used to model the smart window unit's thermal properties and calculate its thermal conductance for different applied temperature conditions. In the second phase, the TT PS-TIM structure with the thermotropic material in both its clear and translucent states were modelled using RADIANCE (Version 4.1). The genBSDF function in RADIANCE was used to obtain accurate optical properties of the window unit, called the Bidirectional Scattering Distribution Function (BSDF). In the third phase, the obtained dynamic thermal properties and the accurate optical properties (i.e. BSDF datasets) with the thermotropic material in both clear and translucent states were input into Energy Plus (Version 9.2.0) to perform building energy simulations. The Energy Management System (EMS) function was used to achieve simulation of the thermotropic materials' dynamic response to the surrounding environment. Once the EnergyPlus simulation was completed, an hourly profile showing the state of the thermotropic layers (i.e. clear state or translucent state) was generated. This was then in the final phase input into RADIANCE as a schedule file to enable further detailed annual daylight simulation.

Table 1
Optical properties of the thermotropic layer in its clear state (CS) and seven modelled translucent states (TS).

		Transmittance	Reflectance	Absorptance
CS		85%	15%	0
#1	TS_{t10r35}	10%	35%	55%
#2	TS_{t20r35} (370 k 5 wt% HPC)	20%	35%	45%
#3	TS_{t30r35}	30%	35%	35%
#4	TS_{t40r35}	40%	35%	25%
#5	TS_{t10r45}	10%	45%	45%
#6	TS_{t30r25}	30%	25%	45%
#7	TS_{t40r15}	40%	15%	45%

2.3. Thermal model through FLUENT

To obtain accurate thermal properties (thermal resistances) of the smart window unit containing TT PS-TIM for use in the resultant building simulation, a validated two-dimensional finite volume model [37,38] developed using the CFD software ANSYS FLUENT 15.0 was used to solve the conductive, convective and radiative heat transfer properties of the system.

During the CFD modelling process, the internal surfaces of the left and right glazing panes were set as two isothermal walls while the top and bottom ends were assumed to be adiabatic. The enclosure was filled with air ($Pr = 0.71$). The fluid density and viscosity vary with temperature while all the other thermophysical properties of the fluid were assumed to be constant. Extensive mesh independence studies and iterative convergence were conducted. A mesh independent solution was attained when further refining of the mesh gives a similar result without considerable difference (i.e. <1%) to the current mesh solution. In the final model, smaller size meshes with dimension 0.025 mm × 0.025 mm were arranged near the two glazing surfaces, which then gradually increased in size towards the centre of the cavity. The modelling method was validated through comparing the simulation results with experimental data obtained from a series of tests conducted in a large climatic chamber (TAS Series 3 LTCL600) at the University of Nottingham, UK. Details about the validation process can be found in the authors' previous publication [37,38]. The boundary conditions of the two isothermal surfaces were set to match 55 temperature scenarios, which represents the commonly encountered conditions experienced in the built environment. In these 55 scenarios, the mean temperature of the two glazing panes ranges from −15 °C to 35 °C and the temperature difference between the two glazing panes ranges from 5 °C to 25 °C.

Based on the simulation results of conductive, convective and radiative thermal transfer of all of these 55 scenarios, a series of equivalent thermal conductivities of the TT PS-TIM structure between these glazing panes were obtained to describe the dynamic conductance under any temperature condition within the tested range. These equivalent thermal conductivities have been further used in EnergyPlus for annual energy performance simulations.

2.4. Optical modelling using RADIANCE

The use of a simple single value of hemispherical solar/visible transmittance, which indicates the total amount of direct and diffuse transmitted or reflected solar energy or daylight flux, is only sufficient for a simple window structure, such as a conventional double-glazed window. For daylight distribution calculations of a complex fenestration system, a more sophisticated measure is required to represent the optical performance. The evaluation of the BSDF can fulfil this requirement by determining coefficients that allow allocation of light from each exterior direction to each interior direction [39,40]. In order to locate each single direction, both incoming and outgoing hemispheres have been discretized into 145 pitches. Each BSDF matrix describes reflectance or transmittance distribution in the outgoing hemisphere for each incident angle of the incoming hemisphere [40,41]. In this research, a raytracing program, genBSDF [42], in RADIANCE was used to characterize the BSDF of the window units with TT PS-TIM based on their geometry and material optical properties. Fig. 4(b)–(j) demonstrates the angularly resolved transmission of the window units with different optical properties using an example of one incident angle (Altitude angle 20°, Azimuth angle 0°) from the incoming hemisphere (shown in Fig. 4(a)). As can be seen in Fig. 4(b) for Double Glazing (DG), scattering of daylight rays cannot be observed. For TT PS-TIM in its clear

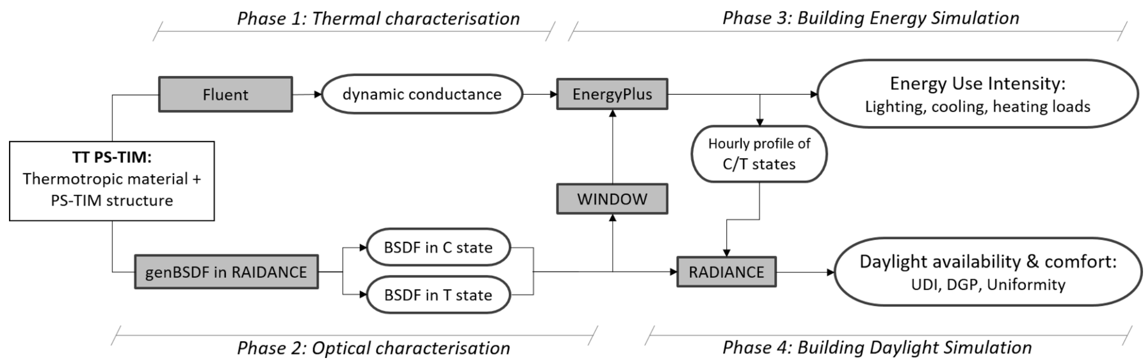

Fig. 3. Flow chart of the workflow for modelling TT PS-TIM window unit.

state, most of the flux is directly transmitted while a small portion of flux is redirected to the upper directions due to the presence of the clear slats (Fig. 4(c)). For TT PS-TIM in their translucent states with different applied optical properties, the transmitted daylight is scattered significantly with considerable redirection of rays when passing through the window system. For window units with TS #1, #2, #3 and #4 (i.e. TS_{t10r35}, TS_{t20r35}, TS_{t30r35} and TS_{t40r35}), with the increase of slat's material transmittance from 10% to 40% (see Table 1), more light predicted to penetrate through the window system into the lower part of the outgoing hemisphere. The hemispherical transmittances of window units #1, #2, #3 and #4, for the specific incident angle (shown in Fig. 4 (a)), are 54.1%, 56.4%, 59.0% and 62.1%, respectively. Window units with TS #5, #2, #6 and #7 (i.e. TS $_{t10r45}$, TS $_{t20r35}$ TS $_{t30r25}$ TS $_{t40r15}$) all have the same absorptance. The decrease of reflectance leads to the increase of transmittance. For these 4 combinations, the overall hemispherical transmittances of these systems, are all the same, 56.4%. This is because the overall hemisphere transmittances is basically a combination of reflectivity and transmittance, as the reflected part of the TT PS-TIM ends up in the room. However, as can be seen in Fig. 4(h) (e) (i) and (j), with the decrease of reflectance, more light rays are transmitted into the lower hemisphere rather than redirected to the upper hemisphere. It is expected that the same amount of transmitted and absorbed solar heat gain may lead to a similar energy profile when used in buildings. However, the different spatial distribution of daylight may lead to different daylight performances when implemented into buildings.

2.5. *Building energy simulations using EnergyPlus*

To demonstrate how the thermotropic material dynamically responds to the ambient environment and how the smart window unit with TT PS-TIM influences the energy performance of an office building, a single office room (2.9 m (width) × 4.4 m(depth) × 3.3 m (height)) was modelled in EnergyPlus and used for analysis in this study. Influences from surrounding buildings, vegetation or other obstructions were ignored. A window of dimensions 1.4 m (height) × 2.9 m (width) was located in the south wall, which was also the only wall exposed to external conditions. The remaining surfaces were assumed to be buffered by mechanically conditioned spaces and therefore experience no inter-zonal heat flow. The building performance simulations were conducted using one-hour time steps for an entire year using the IWEC (International Weather for Energy Calculation) weather data for London, Stockholm, Rome and Singapore. Two occupants were assumed to use this office from 09:00 to 17:00 on weekdays. During these times, standard equipment and lighting loads were assumed to be 13 W/m^2 and 16 W/m^2, respectively [43,44]. A Heating, Ventilation and Air Conditioning (HVAC) system with set points of 25 °C for summer and 21 °C for winter were assumed to operate during occupancy hours.

The resultant dynamic thermal conductance of the smart window unit with TT PS-TIM which was calculated using FLUENT was input into EnergyPlus using the EMS function. Two BSDF datasets of the unit with thermotropic material in both its clear and translucent states were also imported into EnergyPlus. Commands written in EMS were used to control the switching between clear and translucent states. The temperature of the TT slats of the window unit were used at the beginning of each time step to determine if switching would occur. If the TT slats temperate was higher than the specified transition temperate, the BSDF files for the translucent state were applied in the energy balance calculation. Otherwise, the BSDF files for the clear state were applied in the calculation. Based on the internal and external surface temperatures of the tested window used at the beginning of each time step, the corresponding thermal conductivity was selected from the dataset generated using Fluent and subsequently applied in the energy balance calculation process. Once the EnergyPlus simulation was completed, an hourly profile showing the thermotropic material's state at each time step was generated and further used in RADIANCE for annual daylight prediction.

2.6. *Building daylight simulations using RADIANCE*

The three-phase method available in RADIANCE was used in this research for annual dynamic daylight simulation [45]. In this method, the illuminance or luminance at any point of interest inside the room for a time series were computed using the equation: I = VTDS, where V is the view matrix and D is the daylight matrix, describing the external and internal conditions, respectively. Sky matrix (S) is a time series of sky vectors, which is generated by dividing the whole sky into discrete patches, with each patch being assigned an average radiance value for a given time and sky condition. The Transmission matrix (T), characterizes flux output as a function of input for a particular configuration, represented in BSDF. This method provides an accurate and time-efficient way to conduct an annual simulation. Normally, a single transmission matrix is used in annual simulations. But for the thermotropic material, 2 matrices, one for the clear state and one for the translucent state were used. The switch depends on the hourly schedule file output from the EnergyPlus simulations based on window temperature.

3. Results and discussion

Energy and daylight simulations were undertaken for the smart window unit (a double glazing window integrated with TT PS-TIMs between the two glazing panes). The optical properties of the TT materials in their Clear State (CS) were kept constant but varied in their translucent state (Translucent State (TS)) according to Table 1. For the purpose of demonstrating the mechanism through which savings were made, the following window prototypes were modelled and compared: (1) a conventional double gazed window (labelled as *'DG'*); (2) a

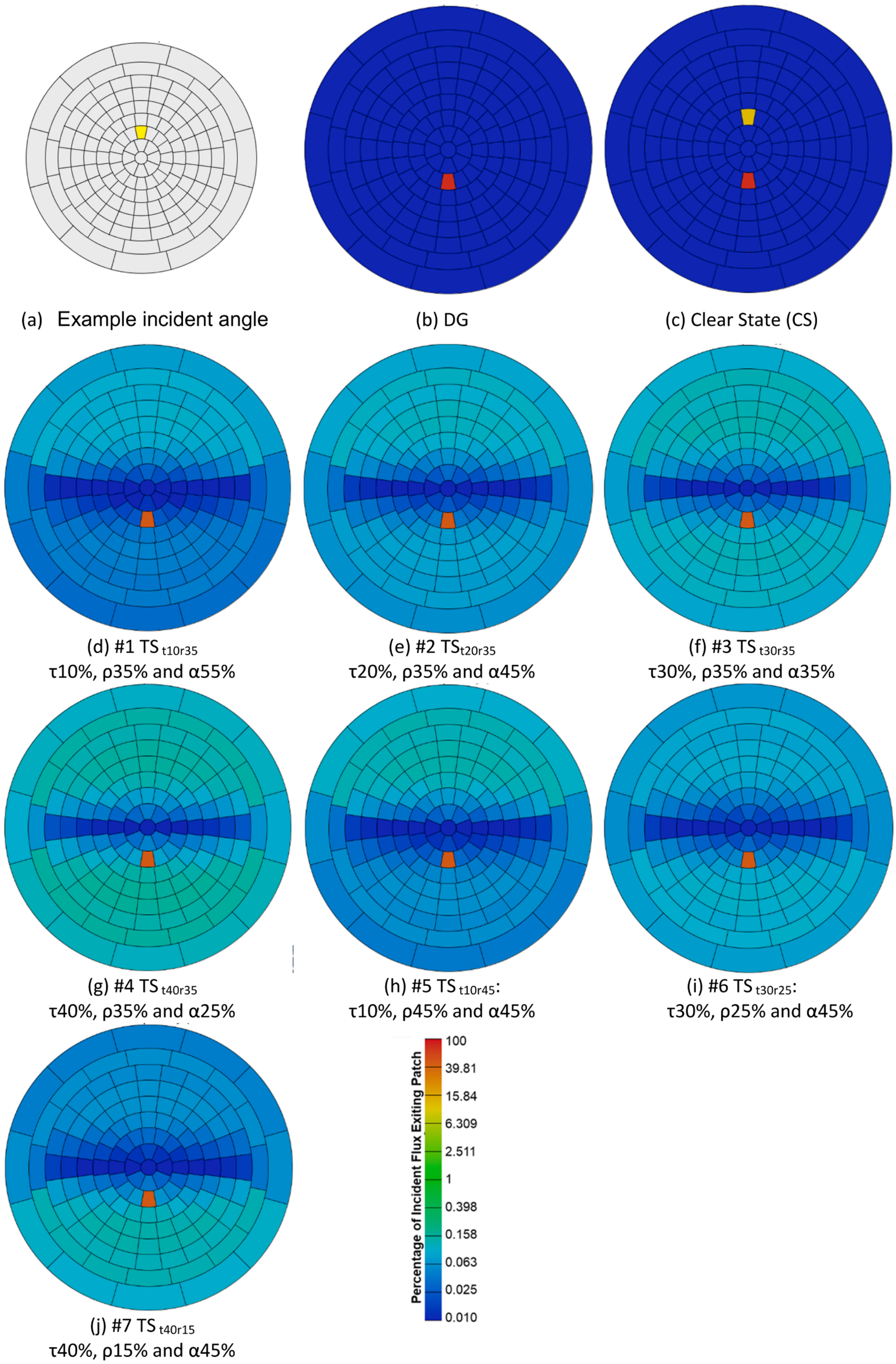

Fig. 4. Predicted BTDFs for the TT PS-TIM window units with different optical properties: an example for one incidence angle.

window with clear PS-TIM, '*C PS-TIM*'; (3) windows with translucent PS-TIMs, '*T PS-TIM*$_{t10r35}$', '*T PS-TIM*$_{t20r35}$', '*T PS-TIM*$_{t30r35}$', '*T PS-TIM*$_{t40r35}$', *T PS-TIM*$_{t10r45}$', '*T PS-TIM*$_{t30r25}$' and '*T PS-TIM*$_{t40r15}$'; and (4) windows with TT PS-TIMs with dynamic slat states shown in Table 1 (i.e. clear and translucent).

3.1. Effect of the thermotropic material's optical properties on their performance

This section evaluates the effect of the thermotropic material's optical properties (the various transmittance, reflectance and absorptance values used for the thermotropic slats are shown in Table 1) on the windows predicted performance and also predicted building performance for a typical cellular office under London climatic conditions. An initial transition temperature of 25 °C for the thermotropic layer was set for the analysis in this section. The transition temperature effects on building performance are evaluated in Section 3.2. In addition, traditional double glazed, windows with static clear and static translucent PS-TIMs are analysed, and their performance compared with TT PS-TIMs.

3.1.1. Effect on window heat gains and switching hours

During the daylight hours, heat gains through the window into the room are dominated by the window solar heat gain augmented by heat transfer resulting due to the temperature difference between the indoor and outdoor environments. The window solar heat gain comprises of solar radiation directly transmitted through the window and secondary heat gains due to the fraction of solar radiation absorbed in the different layers/components of the window and transmitted to the interior by conduction, convection and radiation. To demonstrate how much solar gains are admitted through window systems during working hours throughout the year, hourly window heat gains are plotted against incident solar radiation for the DG, C PS-TIM, T PS-TIM and TT PS-TIM with $CS\text{-}TS_{t20r35}$_25°C and presented in Fig. 5. For the same incident solar radiation intensity on a window surface, if the solar incidence angle is different, the solar thermal energy that is transmitted into the room is different. This leads to the scattering of data points around the trendline. The points are scattered wider for the T PS-TIM_{t20r35} (Fig. 5(c)) and the TT PS-TIM $CS\text{-}TS_{t20r35}$_25°C (Fig. 5(d)) in its translucent state than that for DG (Fig. 5(a)) and C PS-TIM (Fig. 5(b)). This is because the horizontal placed slats in a translucent state allow a larger proportion of solar radiation to be transmitted into the room when the solar incidence angle is low, while redirecting and blocking a larger proportion of solar radiation when the solar incidence angle is high. This is beneficial because the slats can effectively obstruct undesired solar heat flux in the summertime when there is a higher solar incidence angle. The scattering of data points around the trendline is also caused by the changing temperatures between the indoor and outdoor environments. The slope (k) of the trendline represents the ratio of window solar heat gain (including the effects of solar incidence angle and environmental temperatures to incident solar radiation intensity throughout the year, which can be regarded as an annually evaluated Solar Heat Gain Coefficient (SHGC). As can be seen, the SHGC of clear PS-TIM and TT PS-TIM in its clear state is 0.64, which is slightly lower than the static SHGC of DG (i.e. 0.72) due to the presence of the clear slats. Switching TT PS-TIM to its translucent state leads to a considerable reduction of SHGC value from 0.66 to 0.41, which results in less solar heat gain transmitted into the indoor spaces.

The window solar heat gain consists of directly transmitted solar radiation and re-emitted solar radiation that has been absorbed by the window component (i.e. glass panes and TT PS-TIM structure). For the TT PS-TIM with different optical properties for their translucent state, a higher transmittance means larger amounts of direct heat gain while a higher absorptance means a larger capability of the TT layers to absorb solar irradiance. This means larger amounts of secondary solar heat gain. This also increases the window temperature and consequently an increased probability for the TT layer to reach its transition temperature, resulting in more occurrences of switched hours. As indicated in Table 2, with a decrease of solar absorptance in the translucent state of the thermotropic layer from 55% for #1 $CS\text{-}TS_{t10r35}$_25°C to 25% for #4 $CS\text{-}TS_{t40r35}$_25°C, the predicted total annual switched hours decrease from 1080 h to 1010 h. #5 $CS\text{-}TS_{t10r45}$_25°C, #6 $CS\text{-}TS_{t30r25}$_25°C and #7 $CS\text{-}TS_{t40r15}$_25°C all have the same solar absorptance as that of #2 $CS\text{-}TS_{t20r35}$_25°C, so their annual switched hours are the same. For all these simulated TT PS-TIM combinations, as anticipated, most of the switched hours occur in the cooling periods with less than 9 h occuring in the heating periods.

To indicate the effects of the material's optical properties on window heat gain throughout the year, the integrated window heat gain during the heating and cooling periods are illustrated in Fig. 6. Window heating gains during non-cooling or non-heating period are not presented in

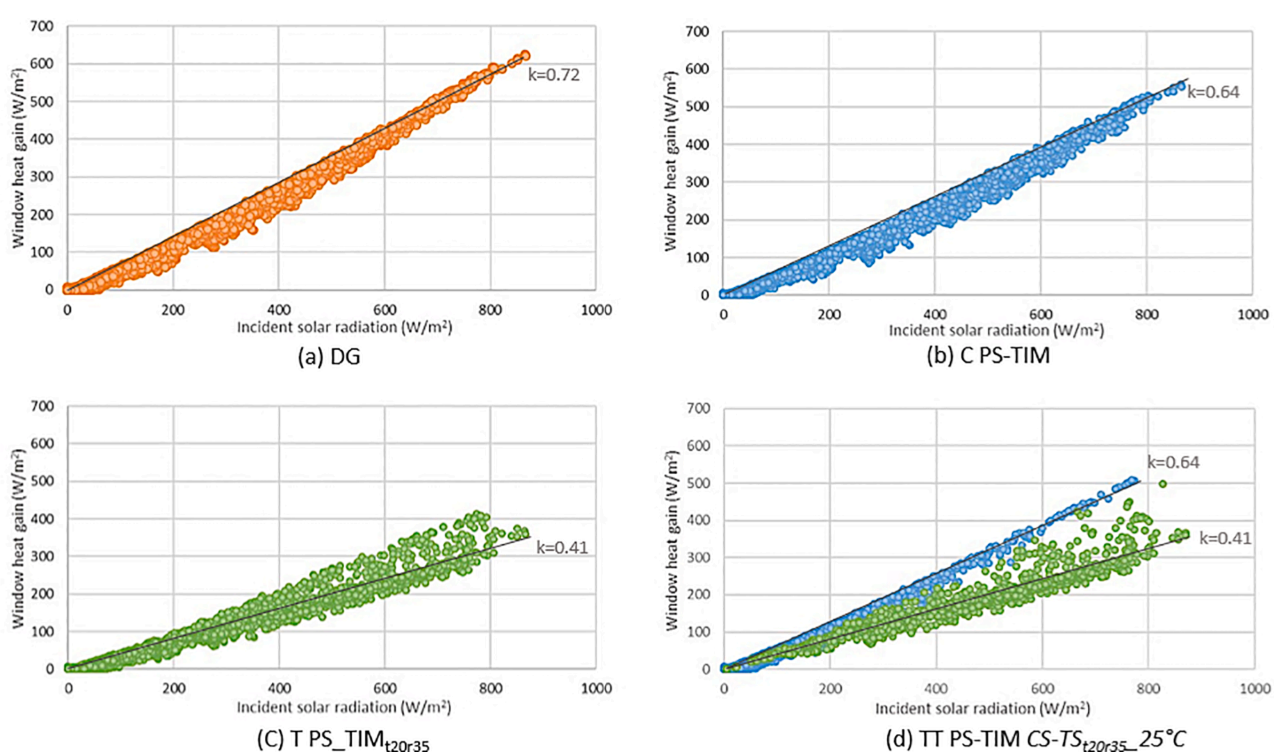

Fig. 5. Predicted Window Solar Heat Gain Coefficients. * *blue points depict the clear state and green points depict the translucent state.* (For interpretation of the references to colour in this figure legend, the reader is referred to the web version of this article.)

Table 2
Predicted annual total switched hours and their distribution in heating and cooling periods.

	#1 CS-TS_{t10r35}_25°C	#2 CS-TS_{t20r35}_25°C	#3 CS-TS_{t30r35}_25°C	#4 CS-TS_{t40r35}_25°C	#5 CS-TS_{t10r45}_25°C	#6 CS-TS_{t30r25}_25°C	#7 CS-TS_{t40r15}_25°C
Total switched hours	**1080**	**1064**	**1041**	**1010**	**1064**	**1064**	**1064**
TT switched hours/total heating hours	**9**/1590	**8**/1591	**8**/1591	**7**/1590	**8**/1591	**8**/1591	**8**/1591
TT switched hours/total cooling hours	**849**/1090	**841**/1089	**827**/1082	**811**/1076	**841**/1089	**841**/1089	**841**/1089

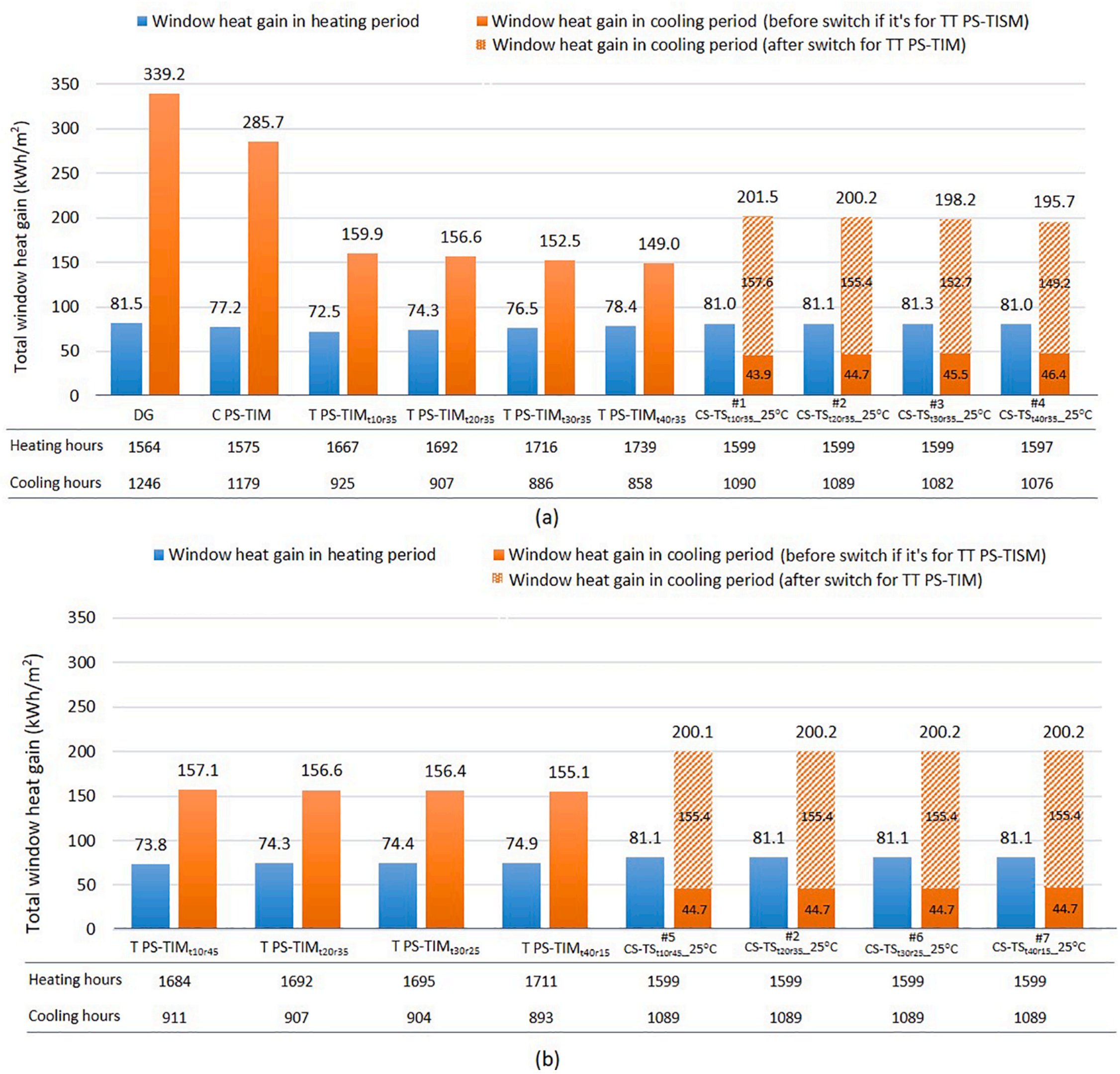

Fig. 6. Predicted accumulated window Heat Gain during heating and cooling periods.

Fig. 6 because they don't affect the building energy consumption in this work. This figure also shows the predicted annual heating hours and cooling hours for these simulated window prototypes. For the first four TT PS-TIM systems (i.e. *CS-*TS_{t10r35}*_25°C*, *CS-*TS_{t20r35}*_25°C*, *CS-*TS_{t30r35}*_25°C* and *CS-*TS_{t40r35}*_25°C*), varying the optical properties of the translucent state for materials #1 to #4, the solar transmittance increases while the solar absorptance decreases. This caused conflicting effects on the window total heat gain. As can be seen in Fig. 6(a), when compared with DG, the presence of PS-TIMs, no matter what sort of material is used, leads to a reduction of solar heat gain and thus an increase in the number of hours that the room required a heating supply and a decrease in the required number of cooling hours. Due to the fact that all the simulated TT PS-TIM window units only switched into their translucent states for a limited proportion of the time when the outdoor temperature was low, the length of the heating period and the total window heat gain in the heating period for these TT PS-TIM window prototypes is almost the same. Applying TT PS-TIM only slightly increases (2%) the heating hours when compared to DG. The resultant window heat gains from TT PS-TIM windows in the heating period, which are beneficial for passive heating, are greater than those from translucent PS-TIM windows. This is evidence that the TT PS-TIM are superior compared to translucent PS-TIM windows in terms of reducing heating demand. The window heat gain from TT PS-TIM windows in cooling periods are significantly lower than that from DG and C PS-TIM and larger than that from T PS-TIM windows. Among the TT PS-TIM windows, #4 '*CS-*TS_{t40r35}*_25°C*' has the most time in its clear state in the cooling period, so its window heat gain in clear state is largest (46.4 Kwh/m^2). This is because all the simulated samples have same properties during clear state, so the accumulated solar heat gain depends on how many hours of them in their clear state during cooling period. However, the window heat gain in their translucent state (i.e. after switching) in the cooling period depends on both the time and the absoptance of TT layer. #4 '$CS\text{-}TS_{t40r35}\_25^{\circ}C$' has the lowest absoptance, thus the shorted hours in translucent state. Meanwhile, the solar heat that absorbed in the slats and further transmitted into rooms has a more profound influence on window heat gain than the direct transmitted solar heat, thus the lowest accumulated heat gains exist for #4 '$CS\text{-}TS_{t40r35}\_25^{\circ}C$'. From a thermal perspective it is beneficial to have a low adsorption as possible as this results in lower heat gains in the cooling period. For TT PS-TIM window unit #5, #2, #6 and #7, as shown in Fig. 6(b), there is no difference between the window heat gains of the different TT PS-TIM window types in both heating and cooling periods. This in effect means that there is no difference between transmittance or reflectance in this model from a thermal point of view. The result proves that varying of solar transmittance against reflectance for the thermotropic slats of PS-TIM does not affect the solar heat gains that pass through the window system integrated with the TT PS-TIM.

3.1.2. Predicted effect on total building energy consumption

This section presents the predicted annual energy consumption of the prototype office when using TT PS-TIM window units with different optical properties. The optical properties of TT PS-TIM system combinations were used according to Table 1. The energy consumption is expressed in terms of kWh/m^2 per year and divided into heating, cooling and lighting energy consumption.

As shown in Fig. 7(a), a clear PS-TIM window system is predicted to only yield an annual energy saving of 4.5% while translucent PS-TIM units ('TS_{t10r35}', 'TS_{t20r35}', 'TS_{t30r35}' and 'TS_{t40r35}') are predicted to provide an annual energy saving potential between 7.9% and 13.8%. The four TT PS-TIM systems are predicted to provide the best overall energy saving potential of all the simulated glazing combinations under the selected London climate, varying from 16.9% to 19.9% if their transition temperature is 25 °C. When compared to the double-glazed unit, the majority of the energy consumption saving is due to significant reductions in cooling energy demands and slight reductions in heating energy demands. For the cooling energy, the saving is achieved through a significant reduction of undesired solar heat gain in the cooling period, which has been discussed in detail in the previous section. There is a small difference between the cooling energy demands of different TT PS-TIM combinations and overall they are slightly higher

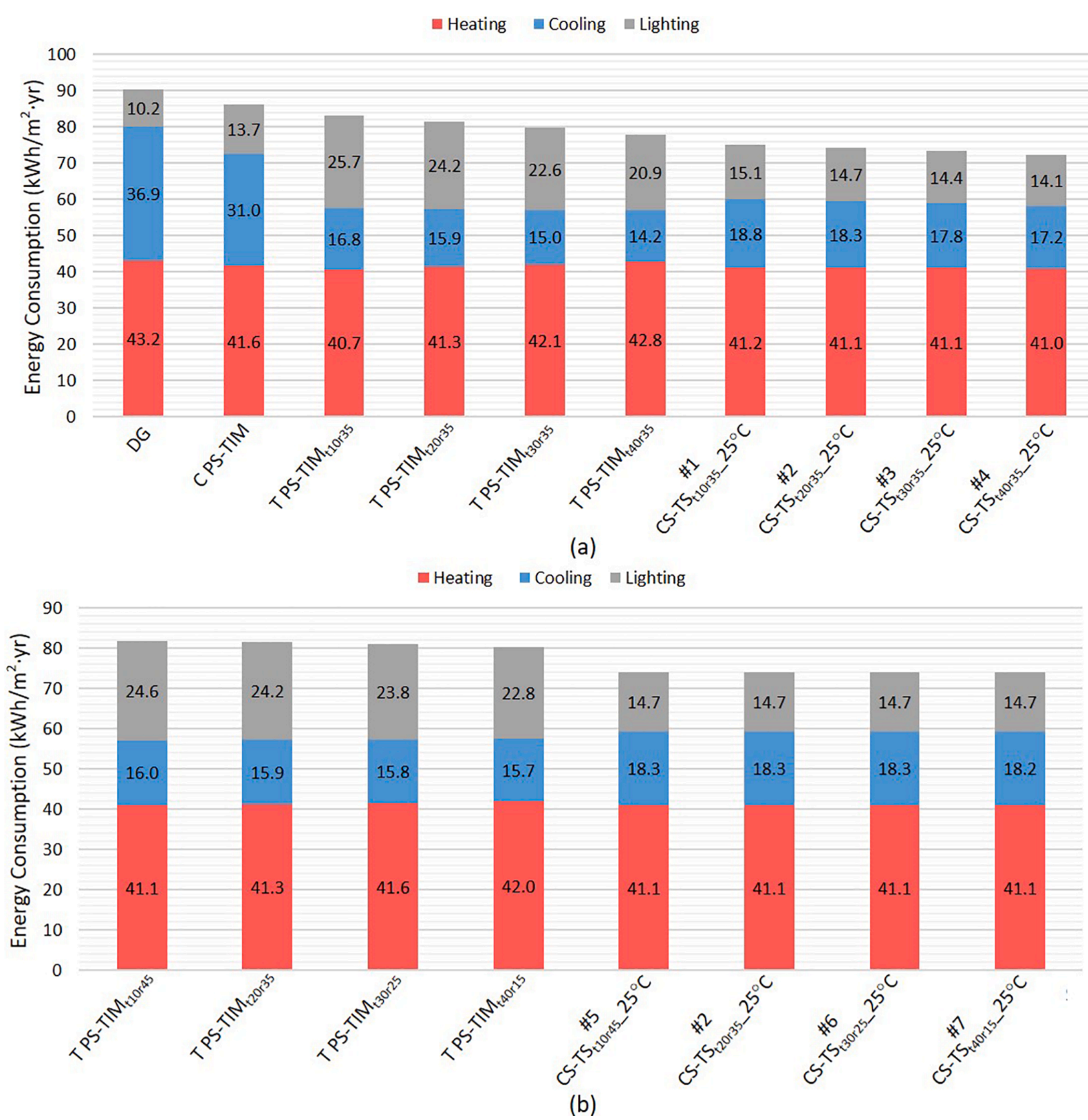

Fig. 7. Predicted annual heating, cooling and lighting energy consumption.

than that of translucent PS-TIM and significantly lower than that of conventional DG and clear PS-TIM. This demonstrates that the thermotropic layers are not switching to their translucent state during all of the working hours in the cooling season (Table 2) but still work effectively for regulating undesired window heat gain during the summertime (cooling season). For the heating energy, saving is achieved through reduced heat loss from the window system because the presence of TT PS-TIM increases window system thermal resistance. All simulated TT PS-TIM systems required a similar heating energy demand as that of the clear PS-TIM. This can be explained by the fact that during the

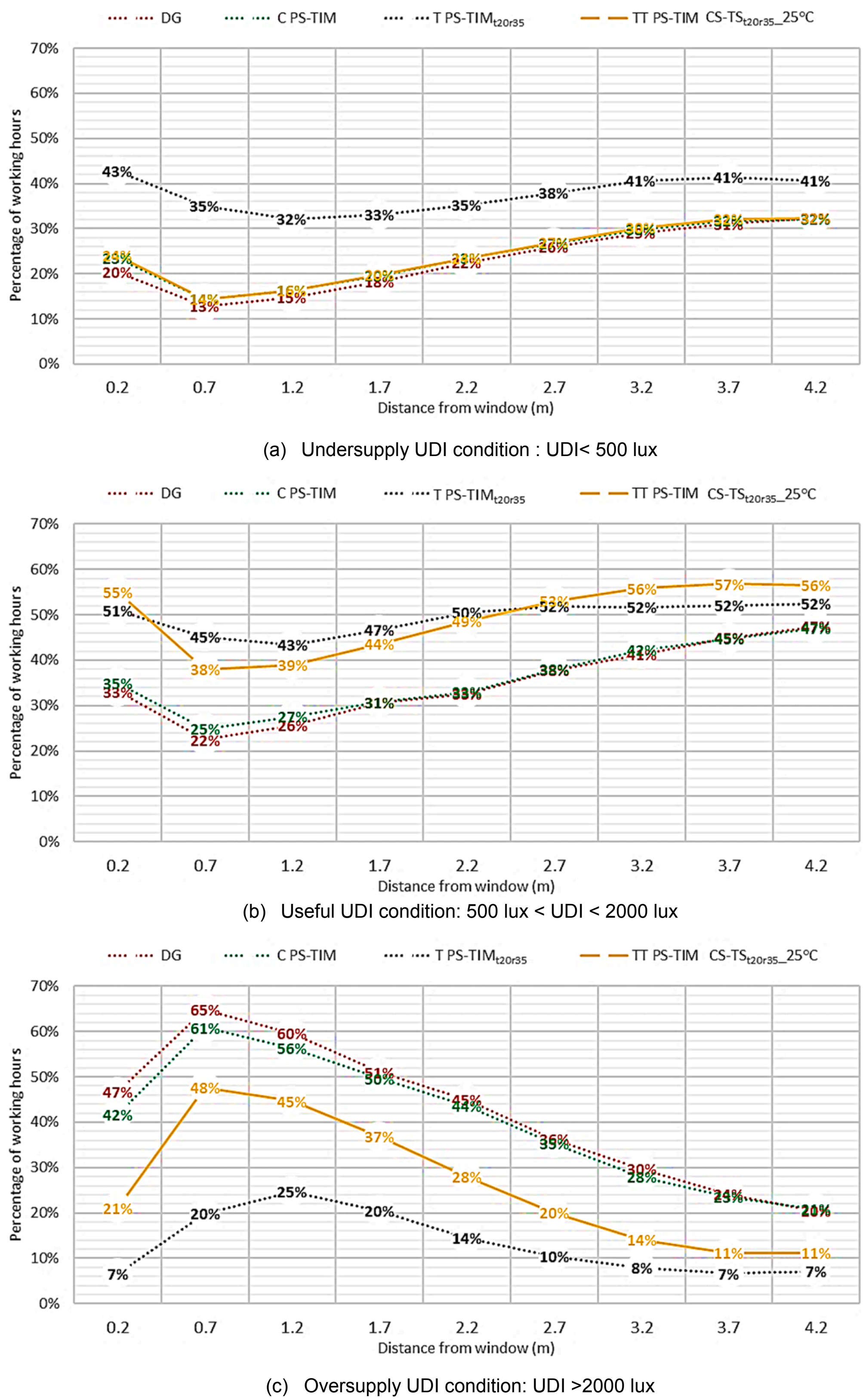

Fig. 8. Predicted UDI distribution in the office for DG, clear PS-TIM, translucent PS-TIM and TT PS-TIM systems.

heating period, the thermotropic layer of TT PS-TIMs are mainly in their clear state. As can be seen in Table 2, the TT layer only switched for less than 9 h in the approx. 1590 h of the heating period for all of the dynamic TT PS-TIM windows modelled. This leads to a negligible difference of required heating energy demand between the TT PS-TIM windows. The lighting energy consumption when applying TT PS-TIM window systems increases when compared to that of DG due to the reduced transmission of daylight. All the TT PS-TIM system combinations are predicted to require slightly higher lighting energy consumption than that of clear PS-TIM and significantly lower than that of translucent PS-TIM. This is evidence that the thermotropic layer could be used to regulate daylight over a period of a year and the requirement to reduce overheating and oversupply of daylight coincide with each other to some extent. Among all the TT PS-TIM systems in this group, adoption of the TT PS-TIM $CS\text{-}TS_{t40r35}\_25^{\circ}C$, which has the highest solar transmittance of 40% and the lowest absorptance of 25% in its translucent state, delivers the lowest heating, cooling, lighting and subsequently overall energy consumption. This can be explained by the fact that the lowest solar absorptance leads to the smallest accumulated solar heat gain transmission during cooling period (see Fig. 6(a)) to yield the lowest cooling energy demand, while a high solar transmittance leads to the largest sunlight transmission, which is beneficial for lighting energy saving.

As shown in Fig. 7(b), it is no surprise to see that there is negligible difference between the heating cooling and lighting energy consumption of applying TT PS-TIM window unit #5, #2, #6 and #7. This is evidence that if the solar absorptance of the TT material's translucent state is fixed, varying the solar transmittance against reflectance does not affect the energy performance of the room it serves.

3.1.3. Predicted effect on daylight environment

Daylight performance of the office space complimentary to the previous window performance and building energy evaluation was assessed using RADIANCE, assuming the office is located in London with the window facing south. The Useful Daylight Illuminance (UDI) metric was used to explore occupant response to varying daylight illumination when simulating TT PS-TIM $CS\text{-}TS_{t20r35}\_25^{\circ}C$ window unit and the *DG*, clear PS-TIM *CS* and translucent PS-TIM TS_{t20r35} counterparts. This is based on simulation of hourly illuminance along the centre line of the room between the window and the end wall. The UDI was determined by sorting the predicted illuminance at the points of interest into 3 bins: an undersupplied bin (illuminance value $<$ 500 lx); a useful bin (500 lx $<$ illuminance value $<$ 2000 lx), where a typical office design illuminance is met and is not exceeded to the point where glare is highly likely; and an oversupplied bin (illuminance value $>$ 2000 lx).

Fig. 8(a)–(c) represent the undersupply UDI, useful UDI and oversupply UDI conditions, respectively along the central line of the office. For a room with a normal south-facing double-glazed window system, over illumination is frequently a problem especially within the region that is close to the window (i.e. periods when the illuminance exceeds 2000 lx account for 45% $-$ 65% of working hours at locations within 2.2 m of the window). The use of a clear PS-TIM *CS* window reduces the predicted oversupplied of daylight by approx. 5% and slightly increases the undersupplied daylight at the area near the window when compared with the DG window, leading to a minor improvement of the daylight availability (i.e. 500 lx $<$ UDI $<$ 2000 lx) near the window. The translucent PS-TIM TS_{t20r35}, which effectively scatters daylight, can significantly eliminate the oversupply of daylight near the window, thus improving the daylighting quality of the room. However, due to the reduced transmittance due to applying translucent PS-TIM, the undersupplied daylight hours increase on average from 23% when the original DG is used to 38%. Because of the dynamic regulating ability of TT PS-TIM, implementing TT PS-TIM provides the benefit of both clear and translucent PS-TIMs. When the illuminance is low, the TT layers of TT PS-TIM structure are always in their clear states. This is deduced by the negligible difference of undersupplied daylight hours (UDI $<$ 500 lx) between TT PS-TIM $CS\text{-}TS_{t20r35}\_25^{\circ}C$ and clear PS-TIM. The TT layers of the PS-TIM structure switch to their translucent state when their temperature is higher than the transition temperature (i.e. 25 °C in this scenario). This happens for a proportion of the working hours when the illuminance is high. Thus, the oversupply of daylight can be effectively reduced to 26% of working hours when implementing TT PS-TIM $CS\text{-}TS_{t20r35}\_25^{\circ}C$. The combined effect of reducing oversupplied daylight and the insignificant change to undersupplied daylight leads to the best performance among all of the simulated window configurations (i.e. the percentage of hours where the UDI is in the useful range increases from 35% for the conventional DG to 50% for the TT PS-TIM). When compared with implementing translucent PS-TIM TS_{t20r35} (49% of working hours are in UDI 500–2000 lx), TT PS-TIM $CS\text{-}TS_{t20r35}\_25^{\circ}C$ provides a higher proportion of working hours that fall into the useful bin for the 1st point near the window and for regions far away from the window ($\geq$2.7 m).

Fig. 9(a) and (b) show the distribution of useful UDI bins (UDI 500–2000 lx), which is used to quantify the daylight performance of TT PS-TIM window systems with different optical properties. The predicted performance of TT PS-TIM window systems #1–#4 are shown in Fig. 9 (a). As can be seen, all the TT PS-TIM prototypes are predicted to provide significant improvement over conventional double-glazing window units. With the transmittance reducing from 40% for #4 $CS\text{-}TS_{t40r35}\_25^{\circ}C$ to 10% for #1 $CS\text{-}TS_{t10r35}\_25^{\circ}C$, the percentage of working hours that fall in the useful range (UDI 500–2000 lx) increases. TT PS-TIM with 1# $CS\text{-}TS_{t10r35}\_25^{\circ}C$, which has the lowest transmittance, gives rise to the highest percentage (i.e, average 52%) of working hours in the useful bin. It also provides the most evenly distributed daylight throughout the room depth as the curve is flattest among the TT PS-TIM combinations. For TT PS-TIM window unit #5, #2, #6 and #7, as shown in Fig. 9(b), there are only minor differences (up to 3%) for the investigated points in the regions that are 0.7 m to 2.2 m away from the window. This result indicates that once the solar absorptance of the TT material's translucent state is kept constant, the variation of solar reflectance and transmittance barely affect the daylight availability of the room it serves.

3.2. Effect of transition temperature on predicted window system performance

In this section, simulations were undertaken for TT PS-TIM window systems of which the TT layer of the slats has fixed optical properties and the transition temperature was set to values between 19 °C and 25 °C. As discussed in the previous section, varying solar transmittance against reflectance while keeping the solar absorptance constant neither affect the energy performance nor daylight performance of applying the TT PS-TIM window system into a building. Thus, TT PS-TIM #5, #6 and #7 are not involved in the following discussion.

3.2.1. Effect of transition temperature on energy performance

Table 3 shows the annual heating, cooling and lighting energy consumption after applying the TT PS-TIM $CS\text{-}TS_{t20r35}$ system with different set transition temperatures of the TT material. The annual switched hours and their distribution in heating, cooling and lighting hours are also shown in Table 3. As can be seen, reducing the transition temperature from 25 °C to 19 °C led to nearly double the total annual switched hours, from 1064 h to 2089 h. When the transition temperature is 19 °C, 9.3% of the switching hours occur in the heating period, which led to an increase in heating energy demand when compared with higher transition temperatures. Meanwhile, the requirement of artificial lighting is also increased to 1853, 565 h of which occur when the TT PS-TIM is switched to its translucent state. Setting the transition temperature at 21 °C and 23 °C can achieve a balance between cooling and lighting energy savings, and thus give rise to the largest potential total energy savings when compared with a conventional double-glazed window. The predicted annual energy performance of TT PS-TIM window #1, #3

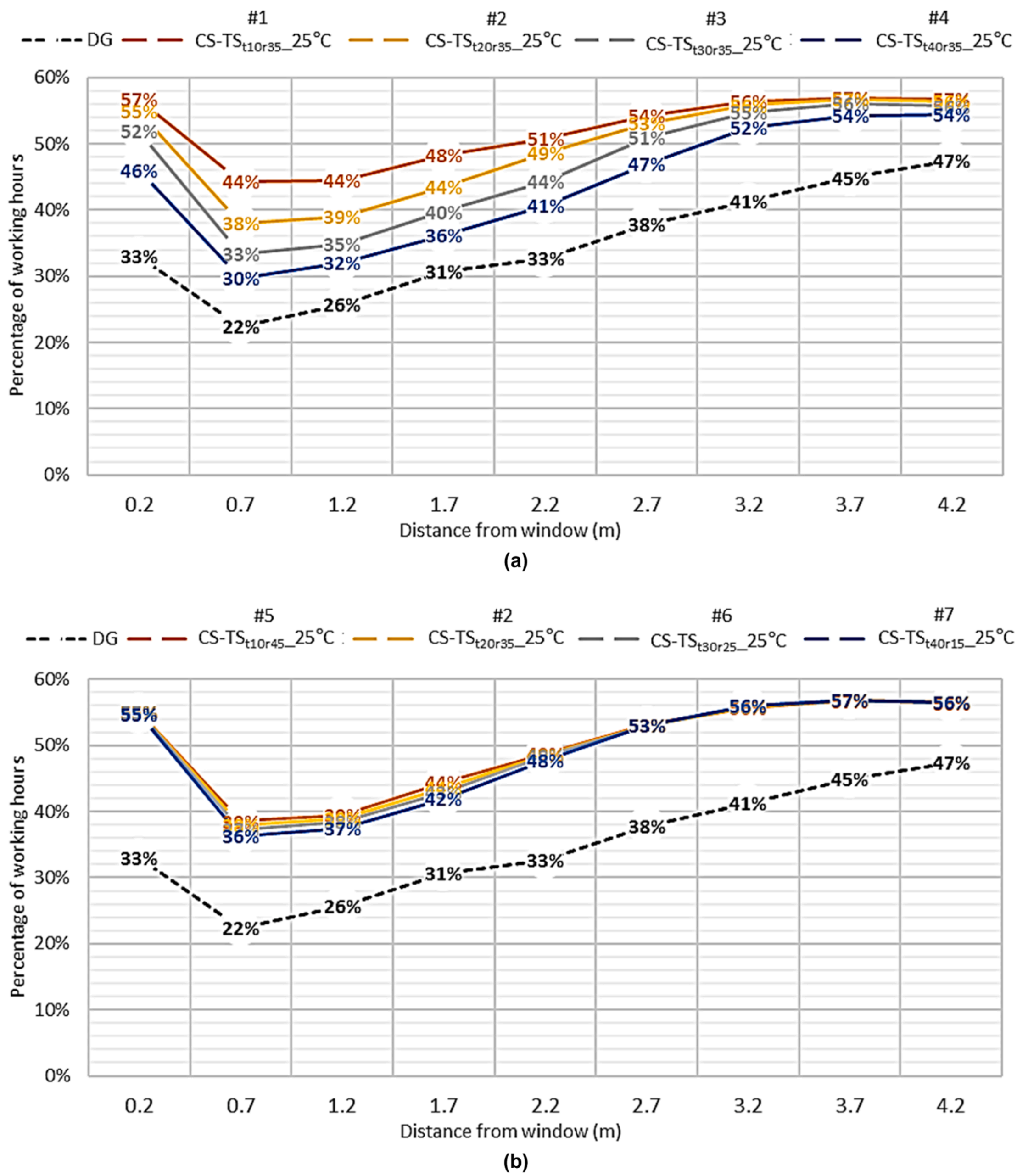

Fig. 9. Predicted useful UDI distribution (500–2000 lx) in the office for TT PS-TIM systems with different optical properties.

Table 3
Predicted office annual energy consumption and TT material switched hours for TT PS-TIM *CS-TS*$_{t20r35}$ with different set transition temperatures.

	DG	*CS-TS*$_{t20r35}$*_19°C*	*CS-TS*$_{t20r35}$*_21°C*	*CS-TS*$_{t20r35}$*_23°C*	*CS-TS*$_{t20r35}$*_25°C*
Total switched hours	–	2089	1696	1355	1064
TT switched hours/total heating hours	–/**1564**	**228**/1697	**67**/1634	**27**/1612	**8**/1591
Heating energy consumption (kWh/m^2)	43.2	42.2	41.6	41.3	41.1
TT switched hours/total cooling hours	–/**1245**	**889**/897	**904**/931	**920**/1009	**841**/1089
Cooling energy consumption (kWh/m^2)	36.9	15.4	15.9	16.7	18.3
TT switched hours/total lighting hours	–/**1156**	**565**/1853	**394**/1787	**289**/1729	**217**/1681
Lighting energy consumption (kWh/m^2)	10.2	16.7	15.7	15.1	14.7
Total saving rate	–	17.8%	19.0%	19.0%	17.9%

and #4 (i.e. *CS-TS*$_{t10r35}$, *CS-TS*$_{t30r35}$ and *CS-TS*$_{t40r35}$) can be found in Table 4. It can be concluded that, a transition temperature of 21–23 °C yields the lowest predicted overall energy demands for all the simulated window combinations. The largest energy saving potential is achieved by applying the window system of *CS-TS*$_{t40r35}$*_21°C*. This leads to an annual energy saving of 21.7% when compared to a double glazed window for the simulated office.

Table 4
Predicted annual energy consumption for window systems TT PS-TIM #1 *CS-TS$_{t10r35}$*, #3 *CS-TS$_{t30r35}$* and #4 *CS-TS$_{t40r35}$* with different set transition temperatures.

	Heating energy consumption (kWh/m^2·yr)	Cooling energy consumption (kWh/m^2·yr)	Lighting energy consumption (kWh/m^2·yr)	Total energy consumption (kWh/m^2·yr)	Energy Saving rate
DG	43.2	36.9	10.2	90.4	
CS-TS$_{t10r35}$_19°C	42.2	16.0	17.6	75.8	16.2%
CS-TS$_{t10r35}$_21°C	41.7	16.4	16.3	74.4	17.7%
CS-TS$_{t10r35}$_23°C	41.4	17.3	15.5	74.2	17.9%
CS-TS$_{t10r35}$_25°C	41.2	18.8	15.1	75.1	16.9%
CS-TS$_{t30r35}$_19°C	42.1	14.8	15.9	72.9	19.3%
CS-TS$_{t30r35}$_21°C	41.5	15.3	15.1	72.0	20.3%
CS-TS$_{t30r35}$_23°C	41.2	16.2	14.7	72.1	20.2%
CS-TS$_{t30r35}$_25°C	41.1	17.8	14.4	73.3	18.9%
CS-TS$_{t40r35}$_19°C	42.0	14.2	15.2	71.5	20.9%
CS-TS$_{t40r35}$_21°C	41.5	14.7	14.6	70.8	21.7%
CS- TS$_{t40r35}$_23°C	41.2	15.6	14.3	71.1	21.3%
CS- TS$_{t40r35}$_25°C	41.0	17.2	14.1	72.3	19.9%

3.2.2. Effect of transition temperature on predicted office daylight environment

Illuminance predictions were made for the TT PS-TIMs with 4 different transition temperatures (19 °C, 21 °C, 23 °C and 25 °C). Fig. 10 (a)–(c) represent the undersupply UDI, useful UDI and oversupply UDI conditions, respectively along the central line of the simulated office when using the TT PS-TIM *CS-TS$_{t20r35}$* window system. As can be seen in Fig. 10(a) for the undersupply UDI bin (UDI < 500 lx), there is a minor difference predicted for different transition temperatures. This indicates that the thermotropic layers with different transition temperatures only switch to their translucent state for a small proportion of working hours when the illuminance level is low. For the oversupplied UDI (UDI > 2000 lx) in Fig. 10(c), with the decrease in transition temperature from 25 °C to 19 °C, the predicted percentage of working hours that fall within the oversupplied bin (i.e. UDI > 2000 lx) reduces. This is because reducing the transition temperature leads to more working hours in which the thermotropic layers are switched to their translucent states, with a reduction in working hours with oversupply of daylight. When working hours in the useful UDI bins of the TT PS-TIM with different transition temperatures were compared with that of the Translucent PS-TIM$_{t20r35}$, it can be concluded that both *CS-TS$_{t20r35}$_19°C* and *CS-TS$_{t20r35}$_21°C* can provide better performance for all the points from the window to the rear of the office.

Fig. 11 shows the useful UDI bins (UDI 500–2000 lx) of TT PS-TIM window systems with different transition temperatures for the other 3 TT PS-TIM series (i.e. #1 *CS-TS$_{t10r35}$* series, #3 *CS-TS$_{t30r35}$* series *and* #4 *CS-TS$_{t40r35}$* series). Overall, for all of these combinations, a lower transition temperature provides a better daylight availability. For #1 *CS-TS$_{t10r35}$* series, when compared with the performance of a static T PS-TIM$_{t10r35}$, once the transition temperature is lower than 23 °C, the TT PS-TIM will provide a better performance for all of the simulated points from the window to the rear of the office. When the transition temperature is 19 °C, the average percentage of hours where the UDI is in the useful range is 58%. This provides the highest daylight availability among all of the tested combinations, which is a significant increase when compared with 23% for that of a conventional double glazed window. For #4 *CS-TS$_{t40r35}$* series, there is limited difference between a transition temperature of 19 °C and 21 °C. Both are able to provide a better performance for all of the simulated points when compared with the performance of a static T *PS-TIM$_{t40r35}$*.

3.3. Sensitivity analysis

As demonstrated in the previous sections, both optical properties and transition temperature of the thermotropic material layer has effects on the final energy efficiency and daylight performance. Regulating the solar or visible transmittance with a fixed reflectance and varying the absorptance in its translucent state has a significant effect on its energy performance, while regulating transmittance through varying reflectance with a fixed absorptance only affects window system daylight performance slightly. Other parameters of the TT PS-TIM model may also affect the building performance. Thus, a sensitivity analysis has been performed using the Morris one-at-a-time (MOAT) method [46] to explore the simulation parameters associated to the TT PS-TIM model and assess how these changes affected the building energy saving potential and average daylight availability [47,48]. The impact of the parameters related to the whole room level, such as Window-to-Wall-Ratio and U-value of the wall were not considered because the sensitivity analysis is focused on the window scale. Four parameters related to the TT PS-TIM models are taken as inputs, which are:

- X1: slat thickness (in the range of 1.2–1.5 mm, where the 0.5 mm TT membrane layer was kept constant and the PMMA sheet thickness varies from 0.35 mm to 0.5 mm);
- X2: slat area-average thermal conductivity (in the range of 0.13–0.16 W/mK);
- X3: slat solar absorptance (in the range of 20–50%);
- X4: slat transition temperature (in the range of 19–25 °C);

The total energy saving potential (%) and the average UDI (%) are used as outputs to decide the magnitude of the sensitivity to the input variables. We discretize the input space with 4 levels (4 trajectories). This provides elementary effect of each input parameter on each output, at the cost of 20 simulations. Indices of (1) mean value of the absolute value of the elementary effects (μ); and (2) standard deviation of the elementary effects (σ) were obtained. The μ and σ values are plotted in Fig. 12. As can be seen from Fig. 12, both slat thickness and thermal conductivity are predicted to have a negligible effect on the building energy saving potential and no effect on the daylight performance. The slats' solar absorptance has a linear effect on the energy saving potential while the transition temperature of the TT membrane is involved in interactions with other input parameters. Both slat solar absorptance and transition temperature of the TT membrane are involved in interactions with other input parameters.

3.4. The effects of the optical properties and transition temperature under various climates

Having simulated the building performance with TT PS-TIM window systems for the climate of London, a further investigation of the TT PS-TIM performance for three different climate scenarios (Stockholm, Rome and Singapore) was performed. Table 5 summarise the energy saving potential when compared with applying conventional DG and average UDI (i.e. 500–2000 lx) performance for the office space using TT PS-TIM windows #1–4 for the range of transition temperatures investigated in section 3.1–3.2. The performance is classified in five coloured

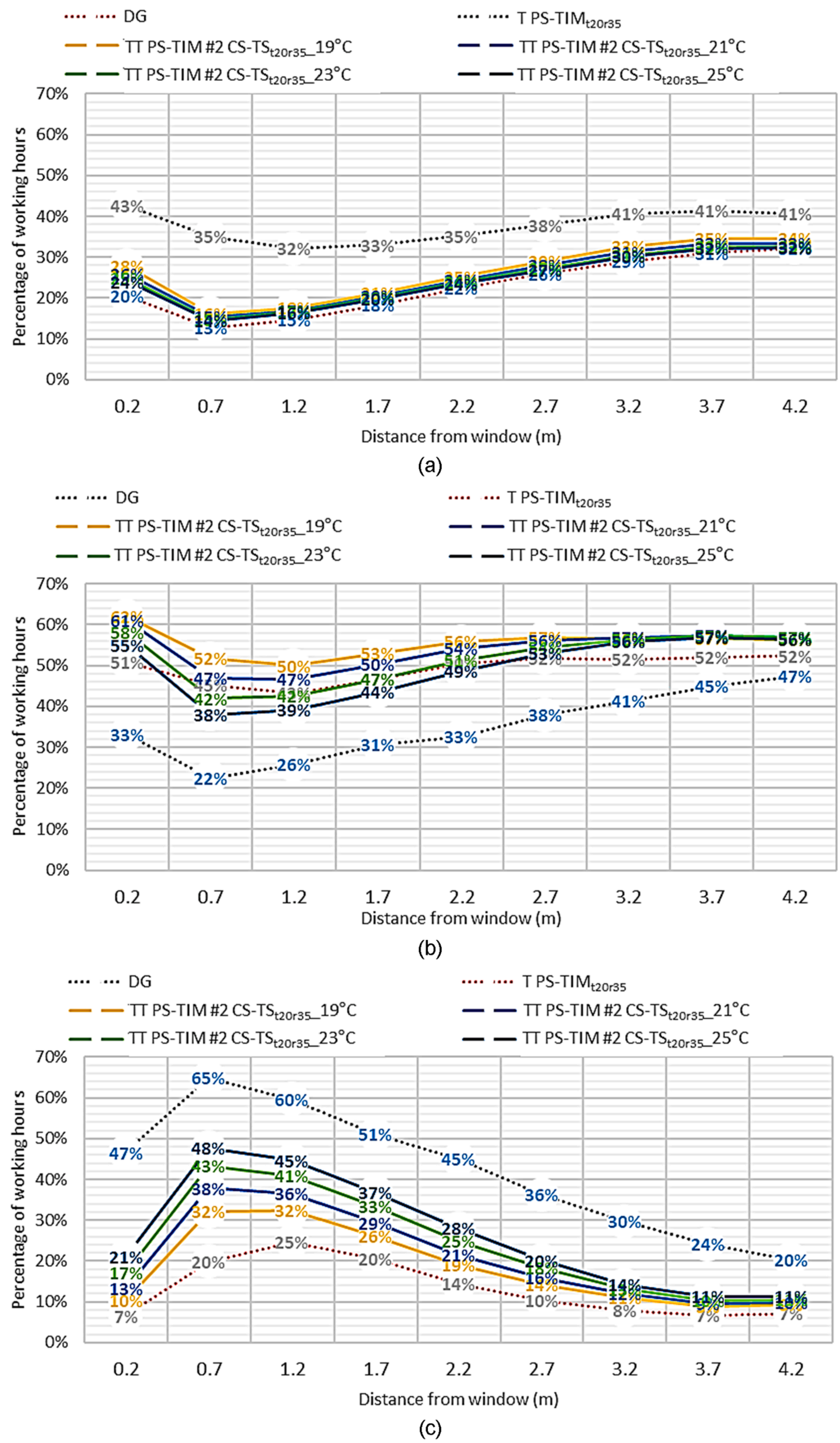

Fig. 10. Predicted percentage of working hours in three UDI bins (a = undersupply, b = useful supply and c = oversupply) distribution for the simulated office with window TT PS-TIM #2 *CS-TS$_{t20r35}$* for 4 different transition temperatures.

bands: dark green (best performing group), light green, yellow, light red, and dark red (worst performing group).

Generally, for simulated locations other than Singapore, the proposed TT PS-TIM windows can provide 16.1–27.1% energy saving when compared with DG. All the TT PS-TIM windows outperformed DG in term of daylight performance as quantified by UDI for all cities. Under the climate of London, the lowest solar absorptance (i.e. #4 *CS-TS$_{t40r35}$*) with a transition temperature of 21 °C yields the lowest energy consumption. From the perspective of achieving highest availability of natural daylight, the system with the lowest translucent-state

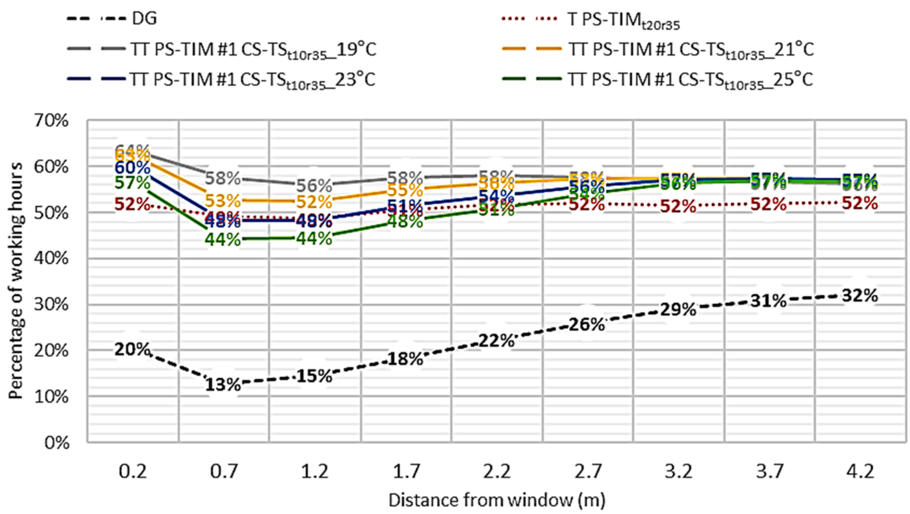

(a)

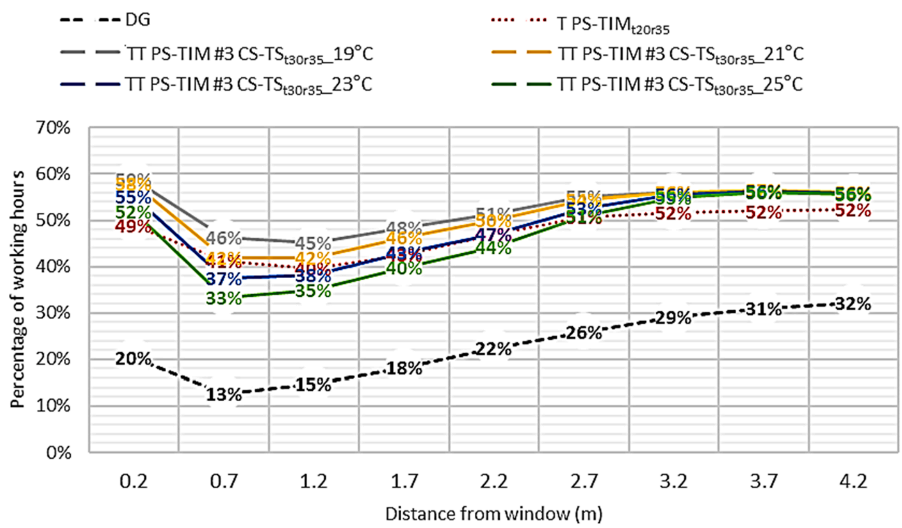

(b)

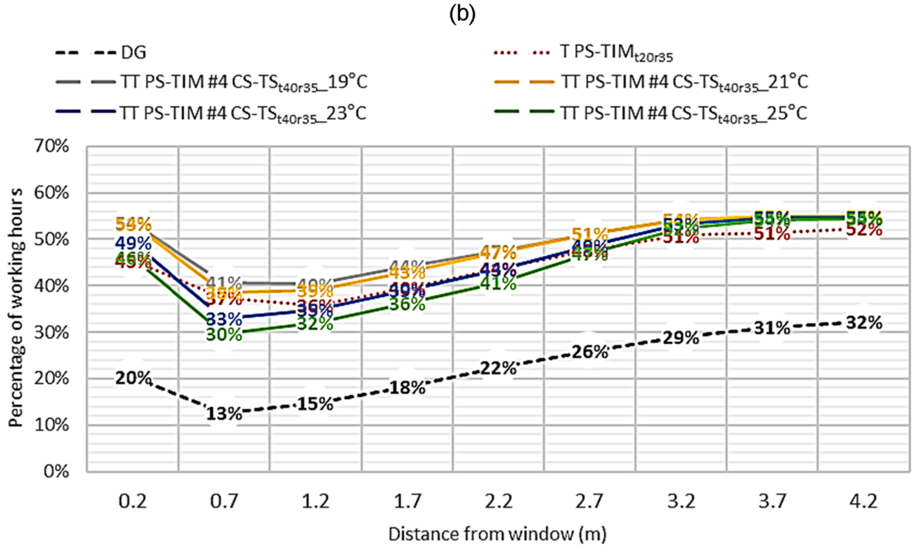

(c)

Fig. 11. Predicted percentage of working hours with useful UDI (500–2000 lx) bin distribution in the office for TT PS-TIM #1 *CS-TS*$_{t10r35}$, #3 *CS-TS*$_{t30r35}$ and #4 *CS-TS*$_{t40r35}$ window systems with varying transition temperatures.

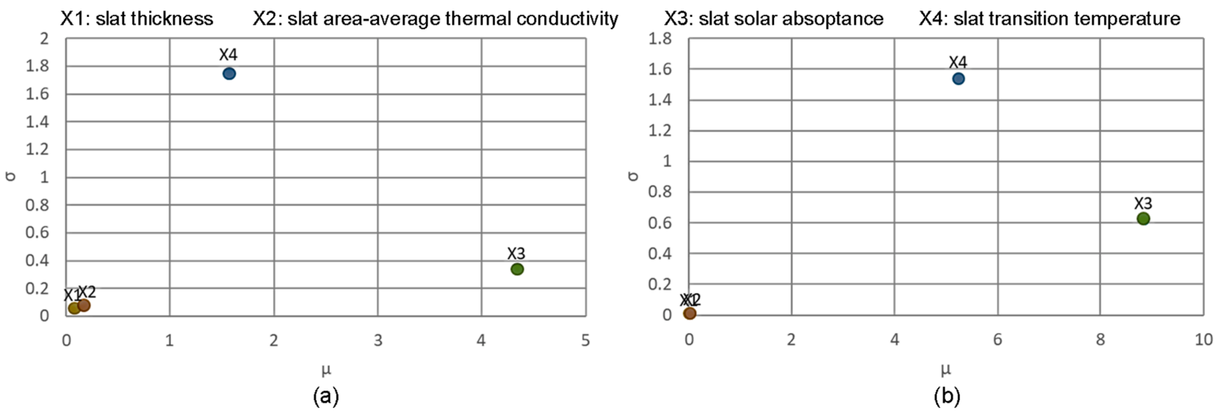

Fig. 12. Results of the MOAT screening: (a) energy saving potential and (b) average UDI.

transmittance (i.e. #1 *CS-TS*$_{t10r35}$) and lowest transition temperature (i. e. 19 °C) can provided the best levels of daylight performance. The system that leads to greatest predicted energy saving potential does not deliver good levels of useful illumination in the office for the climate of London. All of the tested TT PS-TIM window systems show good performance in Rome. The TT PS-TIM with translucent-state transmittance of 40% (i.e. #4 *CS-TS*$_{t40r35}$) provides the greatest energy saving potential and simultaneously good levels (52–52.4%) of daylight availability if its transition temperature is in the range of 19–23 °C. The #1 *CS-TS*$_{t10r35}$ provides the best levels of daylight availability (61.1–62.3%) of all the tested specimens and simultaneously best energy saving potential when the transition temperature is 21 (20%) or 23 °C (20.8%). For the climate of Stockholm, most of the selected TT PS-TIM could not provide satisfactory daylight levels. Under the climate of Singapore, it can be seen that there is no significant difference of the energy and daylight performance between TT PS-TIM with a fixed optical property and varying switching temperature between 19 and 23 °C. This indicates that, the TT material is always in its translucent state, suggesting that a switching temperature between 19 and 23 °C is not suitable for a tropical climate. Finally, it can be concluded that different climates require different optimised designs of TT PS-TIM systems to achieve maximum energy savings and daylight comfort. For cities with extreme climate conditions (e.g. Stockholm and Singapore), the optimised design of a TT PS-TIM system will be investigated in detail in our future research.

4. Conclusion

For the purpose of achieving improved energy efficiency and indoor environment quality, a smart window system, which incorporates a thermotropic material sandwiched between window integrated Transparent Insulation Material slats is under investigation. This smart window system aims to deliver increased thermal resistance as well as dynamic control of solar energy and daylight admission and thus contribute to the international aspirations of reducing building-related CO_2 emissions. To demonstrate this window system's building application and provide guidance for the future steps of material design and development, building simulations of a typical office with Thermotropic Parallel Slat-Transparent Insulation Material (TT PS-TIM) window system prototypes installed for the climates of London, Stockholm, Rome and Singapore have been conducted and presented in this paper. TT PS-TIM systems with varying material properties have been thermally and optically characterised. EnergyPlus and RADIANCE were used for detailed annual performance predictions of energy performance and daylight performance, respectively. Based on the simulation results, the following conclusions can be drawn:

(1) All of the tested TT PS-TIM systems were found to be effective in improving the overall energy efficiency of the room it served, relative to a standard double-glazed system. This is achieved through increased window system thermal resistance reducing

Table 5
Predicted energy saving potential and average UDI for an office space served by TT PS-TIM windows with selected optical properties and switching temperatures for selected city climates.

		Energy saving potential				Average UDI				
		#1 CS-TS$_{t10r35}$	#2 CS-TS$_{t20r35}$	#3 CS-TS$_{t30r35}$	#4 CS-TS$_{t40r35}$	#1 CS-TS$_{t10r35}$	#2 CS-TS$_{t20r35}$	#3 CS-TS$_{t30r35}$	#4 CS-TS$_{t40r35}$	DG
Stockholm	19°C	16.9%	18.3%	19.6%	21.0%	42.2%	40.2%	37.7%	34.6%	26.4 %
	21°C	17.1%	18.5%	19.8%	21.2%	41.5%	39.6%	37.2%	34.1%	
	23°C	16.9%	18.3%	19.6%	20.9%	40.4%	38.5%	36.1%	33.4%	
	25°C	16.1%	17.4%	18.7%	19.9%	39.3%	37.5%	35.3%	32.8%	
London	19°C	16.2%	17.8%	19.3%	20.9%	57.7%	55.4%	52.5%	49.0%	35.1 %
	21°C	17.7%	19.0%	20.3%	21.7%	56.5%	54.0%	51.2%	48.4%	
	23°C	17.9%	19.0%	20.2%	21.3%	54.3%	51.7%	49.0%	45.6%	
	25°C	16.9%	17.9%	18.9%	19.9%	52.1%	49.6%	46.8%	43.6%	
Rome	19°C	19.1%	21.9%	24.5%	26.8%	62.3%	59.9%	56.3%	52.4%	29.4 %
	21°C	20.0%	22.6%	25.0%	27.1%	62.1%	59.7%	56.1%	52.3%	
	23°C	20.8%	23.0%	25.0%	26.9%	61.7%	59.3%	55.8%	52.0%	
	25°C	19.6%	21.7%	23.6%	25.3%	61.1%	58.7%	55.4%	51.6%	
Singapore	19°C	-2.9%	0.1%	2.6%	4.7%	66.8%	67.5%	67.2%	66.1%	38.3 %
	21°C	-2.9%	0.1%	2.6%	4.7%	66.8%	67.5%	67.2%	66.1%	
	23°C	-2.7%	0.2%	2.7%	4.8%	66.8%	67.5%	67.2%	66.1%	
	25°C	0.4%	2.7%	4.6%	6.3%	66.9%	67.6%	67.3%	66.1%	

heating energy demands, as well as dynamic control of undesired solar heat gain to reduce cooling energy demands.

(2) From the perspective of improving daylight performance, applying any of these types of PS-TIM windows could provide significant improvement when compared with a conventional double glazed window. Nearly all of the tested TT PS-TIM prototypes could provide a better average UDI 500–2000 lx than applying static clear or translucent PS-TIM windows. A transition temperature lower than 21 °C provides better UDI 500–2000 lx for all of the simulated points in the office compared to that of applying a static translucent PS-TIM, which has the same optical properties as that of the translucent state of the corresponding TT PS-TIM.

(3) For the simulated scenarios of applying TT PS-TIM window systems for offices subject to the climate of London, the prototype whose thermotropic layer had the lowest absorptance (i.e. $CS\text{-}TS_{t40r35}$) in its translucent state gave rise to the predicted highest energy saving potential of 21.7%. The prototype whose thermotropic layer had the lowest transmittance (i.e. $CS\text{-}TS_{t10r35}$) had the potential to provide the best daylight availability when compared with double glazed windows and other tested TT PS-TIM window prototypes.

(4) Both the optical properties and the transition temperature of the thermotropic material layer impacts the final energy efficiency and daylight performance.

(5) Fixing the solar or visible light reflectance and varying the transmittance and absorptance in the translucent state has a more marked effect on the energy and daylight performance than a fixed absorptance with varying transmittance and reflectance. A lower absorbance leads to a reduction in energy consumption.

(6) A lower transition temperature was shown to provide better daylight performance. However, a transition temperature of around 21 °C results in the best balance between energy demand and daylight provision for the climate of London.

(7) The tested TT PS-TIM systems with 10 mm slat spacing with specified optical properties and switching temperatures ranging from 19 to 25 °C were predicted to provide the greatest energy saving potential and simultaneously good levels of daylight availability for the climate of Rome. Different optimised designs of TT PS-TIM systems are required for different climates.

This paper delivers an insight into optimizing design strategies for novel window units through rigorous numerical modelling, which can assist in the decision-making process for the design of smart windows and their application in real conditions and can thus provide guidance for the next generation of highly energy efficient windows. Future research will be conducted to investigate the quality of view obtained through the proposed configuration of smart window system in detail.

CRediT authorship contribution statement

Yanyi Sun: Conceptualization, Methodology, Software, Validation, Investigation, Writing - original draft. **Xin Liu:** Investigation. **Yang Ming:** Visualization. **Xiao Liu:** Methodology, Validation. **Daniel Mahon:** Writing - review & editing. **Robin Wilson:** Supervision. **Hao Liu:** Supervision. **Philip Eames:** Writing - review & editing. **Yupeng Wu:** Conceptualization, Funding acquisition, Writing - review & editing.

Declaration of Competing Interest

The authors declare that they have no known competing financial interests or personal relationships that could have appeared to influence the work reported in this paper.

Acknowledgements

This work was supported by the Engineering and Physical Sciences Research Council, UK [grant number EP/S030786/1].

References

[1] Pilechiha P, Mahdavinejad M, Pour Rahimian F, Carnemolla P, Seyedzadeh S. Multi-objective optimisation framework for designing office windows: quality of view, daylight and energy efficiency. Appl Energy 2020;261.
[2] Chae YT, Kim J, Park H, Shin B. Building energy performance evaluation of building integrated photovoltaic (BIPV) window with semi-transparent solar cells. Appl Energy 2014;129:217–27.
[3] Sun Y, Shanks K, Baig H, Zhang W, Hao X, Li Y, et al. Integrated semi-transparent cadmium telluride photovoltaic glazing into windows: Energy and daylight performance for different architecture designs. Appl Energy 2018;231:972–84.
[4] Chen X, Yang H, Peng J. Energy optimization of high-rise commercial buildings integrated with photovoltaic facades in urban context. Energy 2019;172:1–17.
[5] Aburas M, Soebarto V, Williamson T, Liang R, Ebendorff-Heidepriem H, Wu Y. Thermochromic smart window technologies for building application: A review. Appl Energy 2019;255.
[6] Peng J, Curcija DC, Thanachareonkit A, Lee ES, Goudey H, Selkowitz SE. Study on the overall energy performance of a novel c-Si based semitransparent solar photovoltaic window. Appl Energy 2019;242:854–72.
[7] Acosta I, Campano MÁ, Molina JF. Window design in architecture: Analysis of energy savings for lighting and visual comfort in residential spaces. Appl Energy 2016;168:493–506.
[8] Huang J, Chen X, Peng J, Yang H. Modelling analyses of the thermal property and heat transfer performance of a novel compositive PV vacuum glazing. Renewable Energy 2020.
[9] Sun Y, Wilson R, Wu Y. A Review of Transparent Insulation Material (TIM) for building energy saving and daylight comfort. Appl Energy 2018;226:713–29.
[10] Sun Y, Liang R, Wu Y, Wilson R, Rutherford P. Glazing systems with Parallel Slats Transparent Insulation Material (PS-TIM): Evaluation of building energy and daylight performance. Energy Build 2018;159:213–27.
[11] Paneri A, Wong IL, Burek S. Transparent insulation materials: An overview on past, present and future developments. Sol Energy 2019;184:59–83.
[12] Wong IL, Eames PC, Perera RS. Energy simulations of a transparent-insulated office façade retrofit in London, UK. Smart Sustainable Built Environ 2012;1(3):253–76.
[13] Sun Y, Liang R, Wu Y, Wilson R, Rutherford P. Development of a comprehensive method to analyse glazing systems with Parallel Slat Transparent Insulation material (PS-TIM). Appl Energy 2017;205:951–63.
[14] Huang Y, Niu J-L. Application of super-insulating translucent silica aerogel glazing system on commercial building envelope of humid subtropical climates – Impact on space cooling load. Energy 2015;83:316–25.
[15] Garnier C, Muneer T, McCauley L. Super insulated aerogel windows: Impact on daylighting and thermal performance. Build Environ 2015;94:231–8.
[16] Sun Y, Wu Y, Wilson R. Analysis of the daylight performance of a glazing system with Parallel Slat Transparent Insulation Material (PS-TIM). Energy Build 2017; 139:616–33.
[17] Zhang Y, Tso CY, Iñigo JS, Liu S, Miyazaki H, Chao Christopher YH, et al. Perovskite thermochromic smart window: Advanced optical properties and low transition temperature. Appl Energy 2019;254.
[18] Ghosh A, Norton B, Duffy A. Behaviour of a SPD switchable glazing in an outdoor test cell with heat removal under varying weather conditions. Appl Energy 2016; 180:695–706.
[19] Flor J-F, Liu D, Sun Y, Beccarelli P, Chilton J, Wu Y. Optical aspects and energy performance of switchable ethylene-tetrafluoroethylene (ETFE) foil cushions. Appl Energy 2018;229:335–51.
[20] Ghosh A, Norton B, Duffy A. Measured overall heat transfer coefficient of a suspended particle device switchable glazing. Appl Energy 2015;159:362–9.
[21] Ghosh A, Norton B, Duffy A. Measured thermal performance of a combined suspended particle switchable device evacuated glazing. Appl Energy 2016;169: 469–80.
[22] Liang R, Sun Y, Aburas M, Wilson R, Wu Y. An exploration of the combined effects of NIR and VIS spectrally selective thermochromic materials on building performance. Energy Build 2019;201:149–62.
[23] Liang R, Liu D, Sun Y, Luo X, Grant D, Walker G. Investigation of Mg-Y coated gasochromic smart windows for building applications. Build Simul 2018;12(1): 99–112.
[24] Piccolo A, Simone F. Effect of switchable glazing on discomfort glare from windows. Build Environ 2009;44(6):1171–80.
[25] Connelly K, Wu Y, Chen J, Lei Y. Design and development of a reflective membrane for a novel Building Integrated Concentrating Photovoltaic (BICPV) 'Smart Window' system. Appl Energy 2016;182:331–9.
[26] Wu Y, Connelly K, Liu Y, Gu X, Gao Y, Chen GZ. Smart solar concentrators for building integrated photovoltaic façades. Sol Energy 2016;133:111–8.
[27] Resch K, Wallner GM. Thermotropic layers for flat-plate collectors—A review of various concepts for overheating protection with polymeric materials. Sol Energy Mater Sol Cells 2009;93(1):119–28.
[28] Wallner GM, Resch K, Hausner R. Property and performance requirements for thermotropic layers to prevent overheating in an all polymeric flat-plate collector. Sol Energy Mater Sol Cells 2008;92(6):614–20.

[29] Resch-Fauster K, Weber A, Holper S, Grobbauer M. Thermotropic overheating protection for façade-integrated solar thermal collectors. Sol Energy Mater Sol Cells 2017;170:39–47.
[30] Inoue T, Ichinose M, Ichikawa N. Thermotropic glass with active dimming control for solar shading and daylighting. Energy Build 2008;40(3):385–93.
[31] Allen K, Connelly K, Rutherford P, Wu Y. Smart windows—Dynamic control of building energy performance. Energy Build 2017;139:535–46.
[32] Yao J, Zhu N. Evaluation of indoor thermal environmental, energy and daylighting performance of thermotropic windows. Build Environ 2012;49:283–90.
[33] Bianco L, Goia F, Serra V, Zinzi M. Thermal and Optical Properties of a Thermotropic Glass Pane: Laboratory and In-Field Characterization. Energy Procedia 2015;78:116–21.
[34] Liu X, Wu Y. Monte-Carlo optical model coupled with inverse adding-doubling for building integrated photovoltaic smart window design and characterisation. Sol Energy Mater Sol Cells 2021;223:110972.
[35] Nishio Y, Chiba R, Miyashita Y, Oshima K, Miyajima T, Kimura N, et al. Salt addition effects on mesophase structure and optical properties of aqueous hydroxypropyl cellulose solutions. Polym J 2002;34(3):149–57.
[36] Wang M, Gao Y, Cao C, Chen K, Wen Y, Fang D, et al. Binary solvent colloids of thermosensitive poly(N-isopropylacrylamide) microgel for smart windows. Ind Eng Chem Res 2014;53(48):18462–72.
[37] Sun Y, Wu Y, Wilson R, Sun S. Thermal evaluation of a double glazing façade system with integrated Parallel Slat Transparent Insulation Material (PS-TIM). Build Environ 2016;105:69–81.
[38] Sun Y, Wu Y, Wilson R, Lu S. Experimental measurement and numerical simulation of the thermal performance of a double glazing system with an interstitial Venetian blind. Build Environ 2016;103:111–22.
[39] Saxena M, Ward G, Perry T, Heschong L, Higa R. Dynamic RADIANCE – Predicting annual daylight with variable fenestratio optics using BSDFs. In: Fourth National Conference of IBPSA-USA. New York City, USA; 2010.
[40] Konstantoglou M, Jonsson J, Lee E. Simulating complex window systems using BSDF data. In: 26th conference on passive and low energy architecture. Quebec City, Canada; 2009.
[41] de Boer J. Modelling indoor illumination by complex fenestration systems based on bidirectional photometric data. Energy Build 2006;38(7):849–68.
[42] Ward G, Shakespeare R. Rendering with radiance: the art and science of lighting visualization, Revised ed. BookSurge, LLC; 2004.
[43] IEA and ECBCS, Annex 45 Energy Efficient Electric: ighting for Buildings: Lighting energy in buildings in Guidebook on Energy Efficient Electric Lighting for Buildings, Liisa Halonen. Eino Tetri, Bhusal P, editors. France; 2006.
[44] Sheppy M, Gentile-Polese L, Gould S. Plug and process loads capacity and power requirements analysis. U.S. Department of Energy; 2014.
[45] McNeil A. The three-phase method for simulation complex fenestration with radiance; 2014.
[46] Morris MD. Factorial sampling plans for preliminary computational experiments. Technometrics 1991;33(2):161–74.
[47] Heiselberg P, Brohus H, Hesselholt A, Rasmussen H, Seinre E, Thomas S. Application of sensitivity analysis in design of sustainable buildings. Renewable Energy 2009;34(9):2030–6.
[48] Pandey B, Banerjee R, Sharma A. Coupled EnergyPlus and CFD analysis of PCM for thermal management of buildings. Energy Build 2021;231.